

**Thermo-Calc
Software**

TC-Prisma Online Training Course

April 23 - 24, 2024

Åke Jansson, Qing Chen



www.thermocalc.com

Day 1: TC-PRISMA (Precipitation Module)

09:00	Software Basics
09:30	Examples: Al alloys
10:20	Q & A
10:35	Theoretical Background: Nucleation
11:00	Examples: Cu alloys
11:45	Q & A

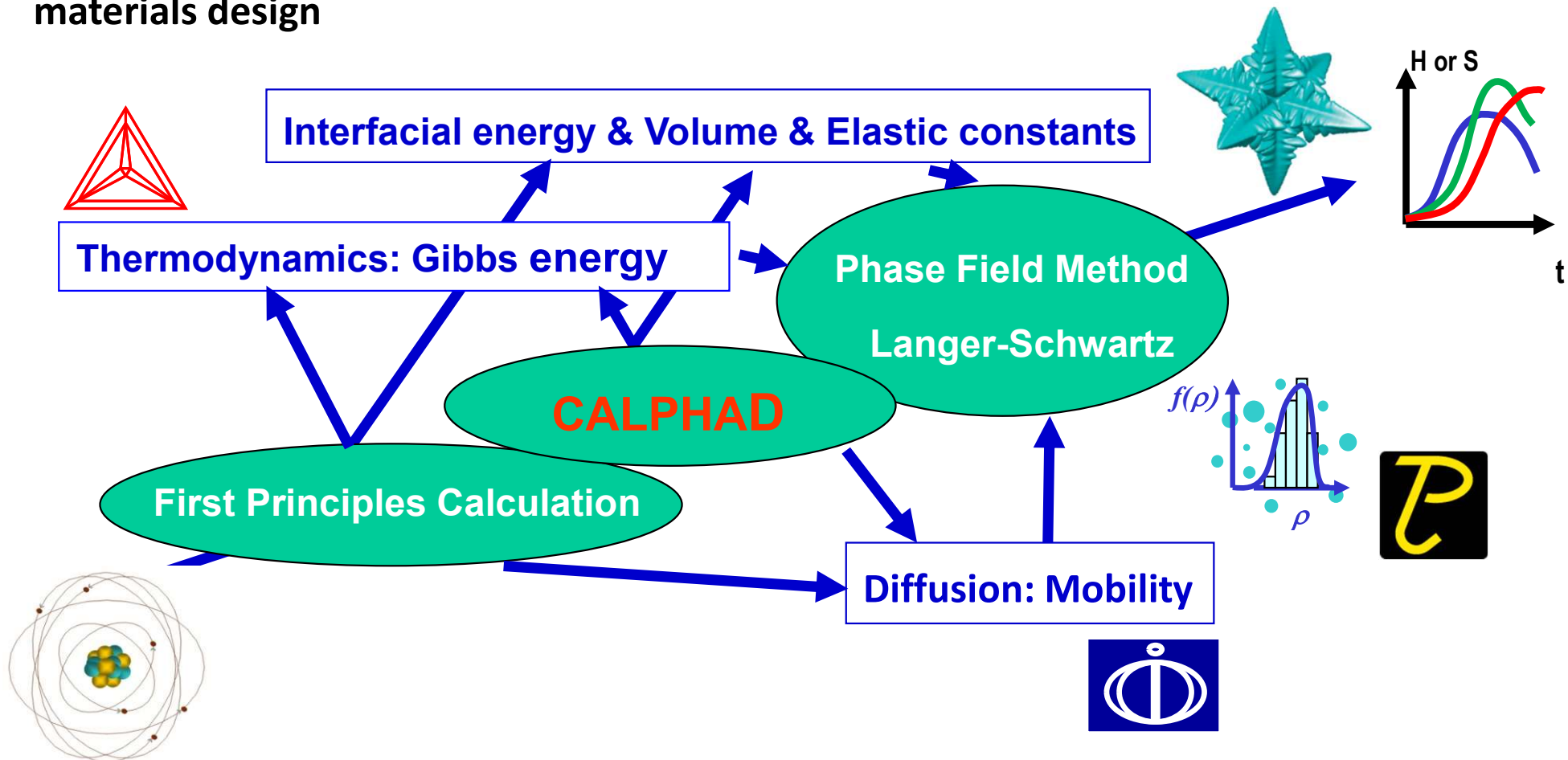
Day 2: TC-PRISMA (Precipitation Module)

09:00	Theoretical Background: Growth Models
09:30	Examples: Ni alloys
10:20	Q & A
10:35	Examples: Steel
11:20	Example: Para-equilibrium
11:45	Q & A

Software Basics

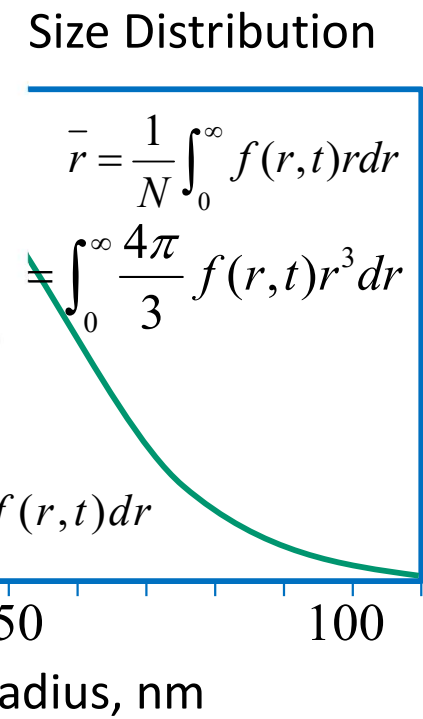
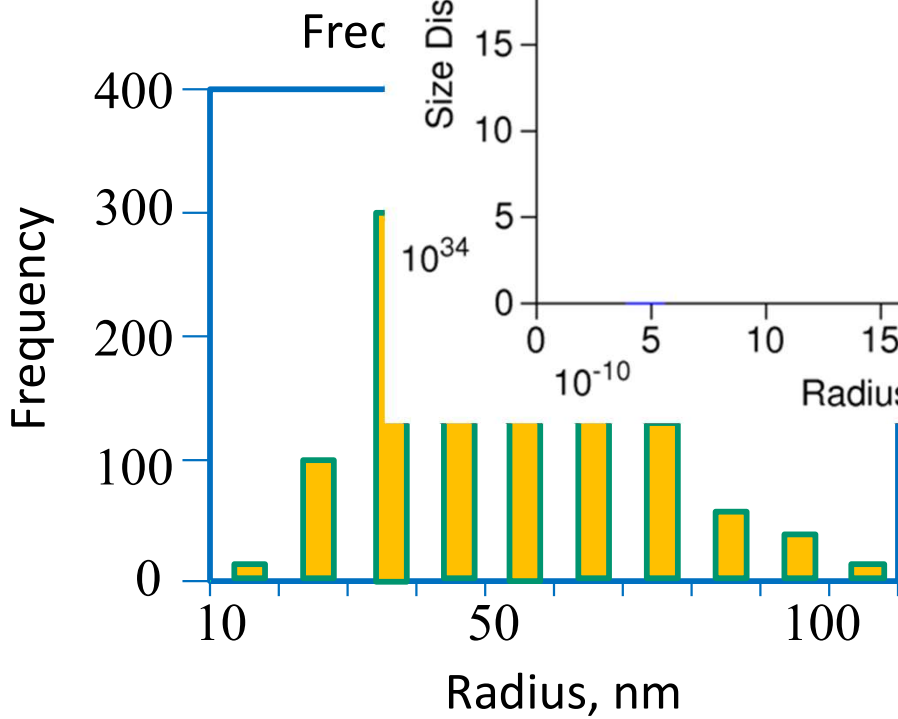
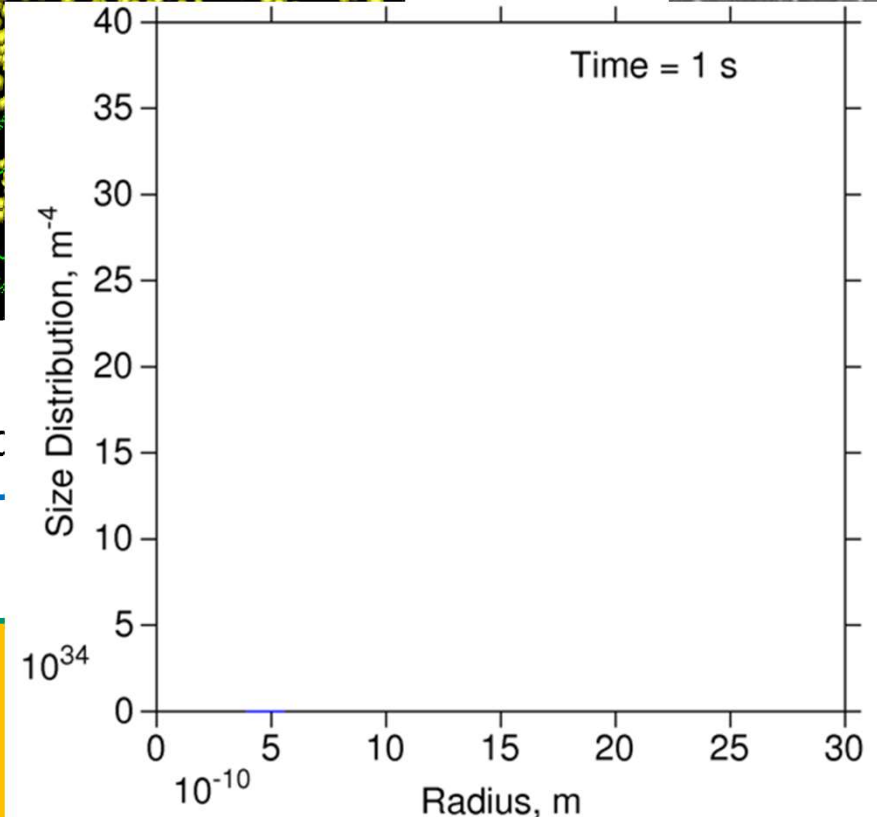
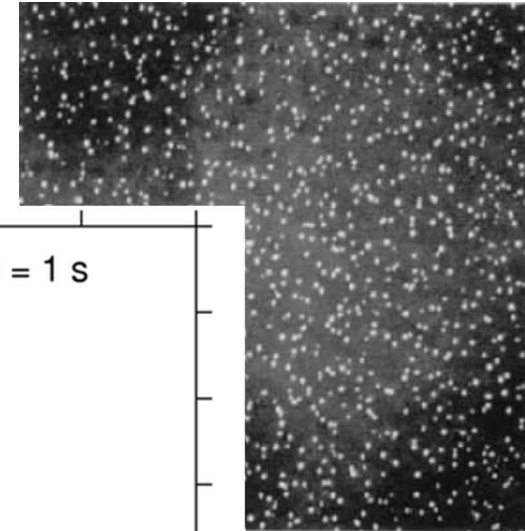
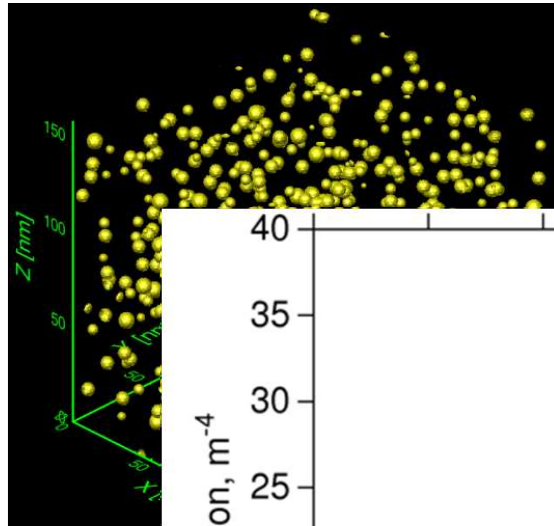
Introduction

CALPHAD method and CALPHAD-based tools play a central role in materials design



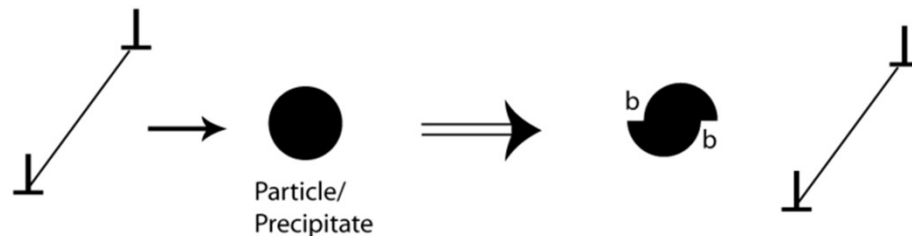
CALPHAD-type databases where each phase is described separately using models based on physical principles and model parameters assessed from experimental and ab initio data provide fundamental inputs for predicting microstructure evolution and materials properties.

Introduction - Precipitation

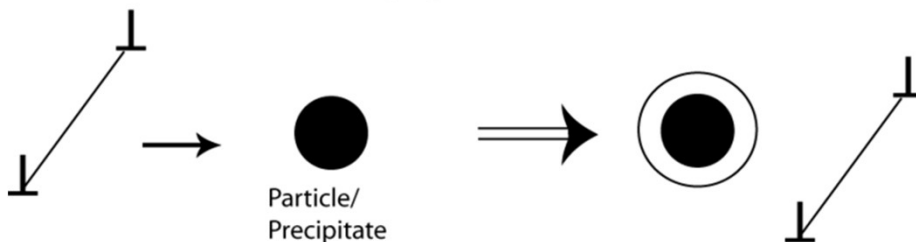


Introduction – Precipitation Hardening

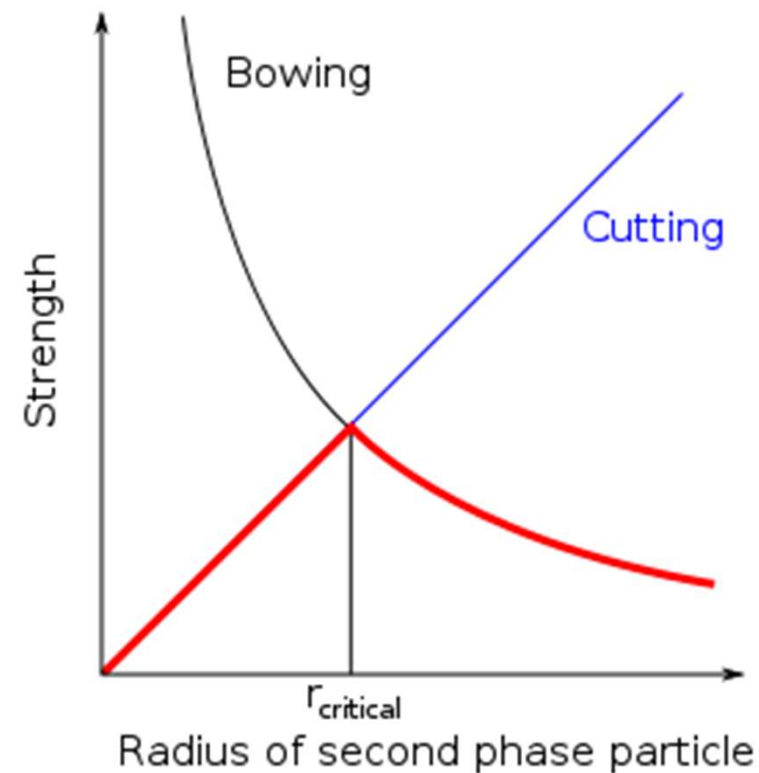
Particle Cutting



Particle Looping



A Simple
Microstructure-Property Model



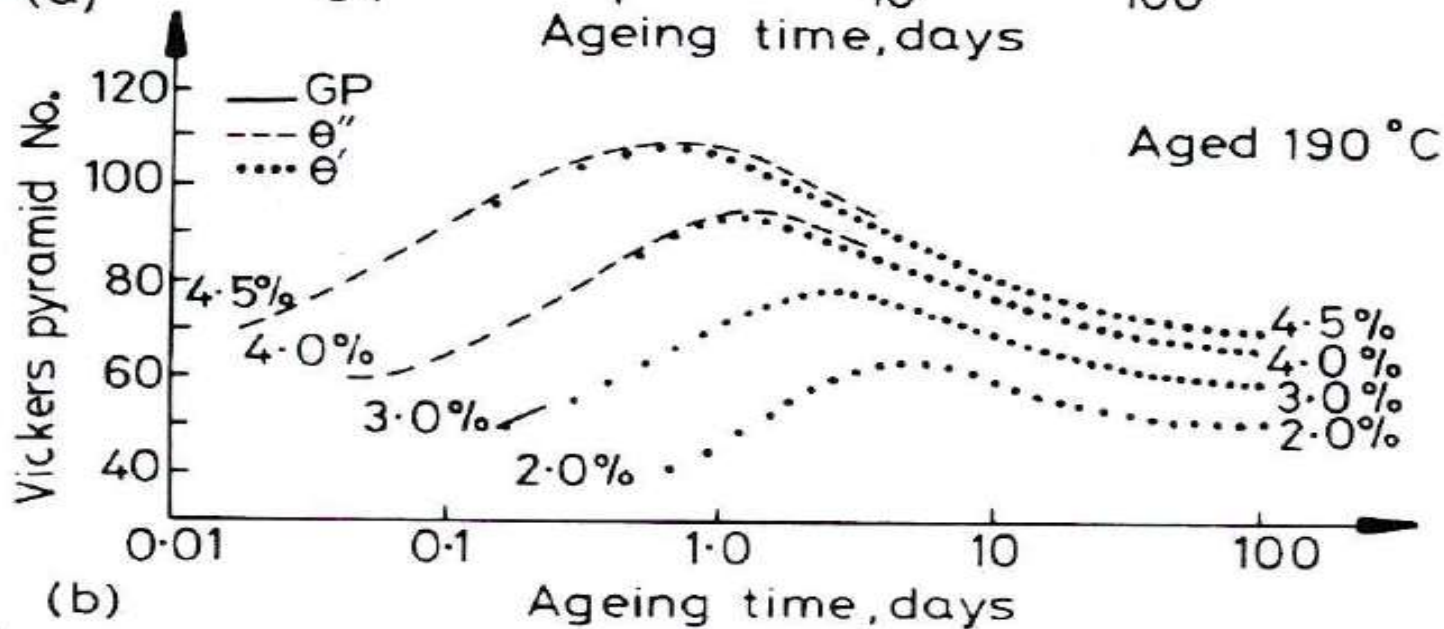
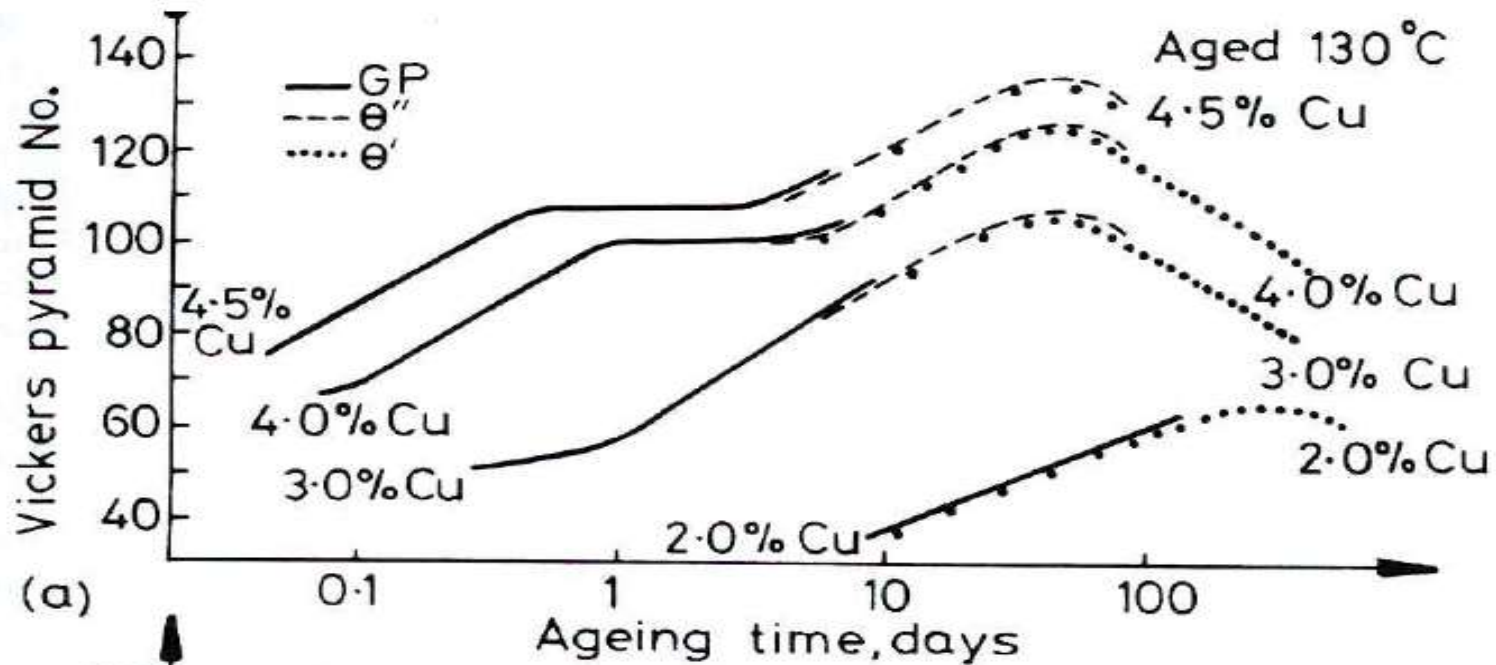
$$\tau = \frac{\pi r \sigma}{bL}$$

r: particle radius
 σ : interfacial energy
 β : Burgers vector
 L: particle spacing
 G: shear modulus

$$\tau = \frac{Gb}{L - 2r}$$

Precipitation hardening, Wikipedia

Precipitation Hardening



[1992, Porter and Easterling, Phase Transformation in metals and alloys]

Approaches to Multi-Particle Precipitation Modeling

- Continuum Models
 - Single-State Models (Volume Fraction or Particle Size)— JMAK Type Model, LSW Coarsening Theory
 - *Two-State Models (Number Particle Density and Particle Size)— LS (Langer-Schwartz) Theory, Cluster Dynamics*
 - Multi-State Models (+ Particle Morphology) — Diffuse Interface (Phase Field) Models, Sharp Interface (Level Set, Boundary Integral, etc.) Models
- Discrete Models
 - Atomistic Models — Kinetic Monte Carlo, Molecular Dynamics

Computational Cost

A vertical black arrow pointing downwards, indicating that the computational cost increases from the top of the list (Continuum Models) to the bottom (Discrete Models).

TC-PRISMA A general computational tool for simulating kinetics of diffusion controlled multi-particle precipitation process in multi-component and multi-phase alloy systems. TC-PRISMA is based on Langer-Schwartz theory [1], and it adopts Kampmann-Wagner numerical (KWN) method [2] to compute the concurrent nucleation, growth, and coarsening of dispersed phase(s).

[1] Langer J, Schwartz A. Phys. Rev. A 1980;21:948-958.

[2] Wagner R, Kampmann R. Homogeneous Second Phase Precipitation. In: Haasen P, editor. Materials Science and Technology: A Comprehensive Treatment. Weinheim: Wiley-VCH, 1991. p. 213.

TC-PRISMA

2011

Version 1.0

- Link to Thermo-Calc and DICTRA
- Multicomponent Nucleation and Growth
- Different Nucleation types
- Advanced Model for Cross Diffusion and High Supersaturation
- Highly Intuitive GUI

2013

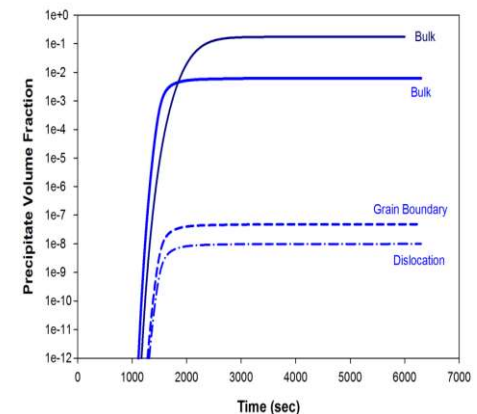
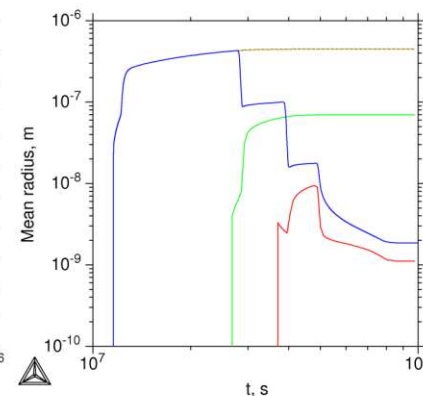
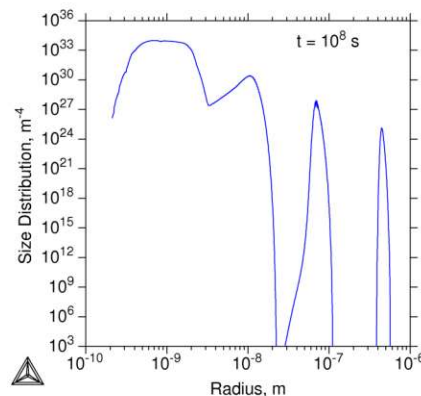
Version 2.0

- Non-Isothermal Conditions
- Multi-Modal PSD Analysis
- Interfacial Energy Model

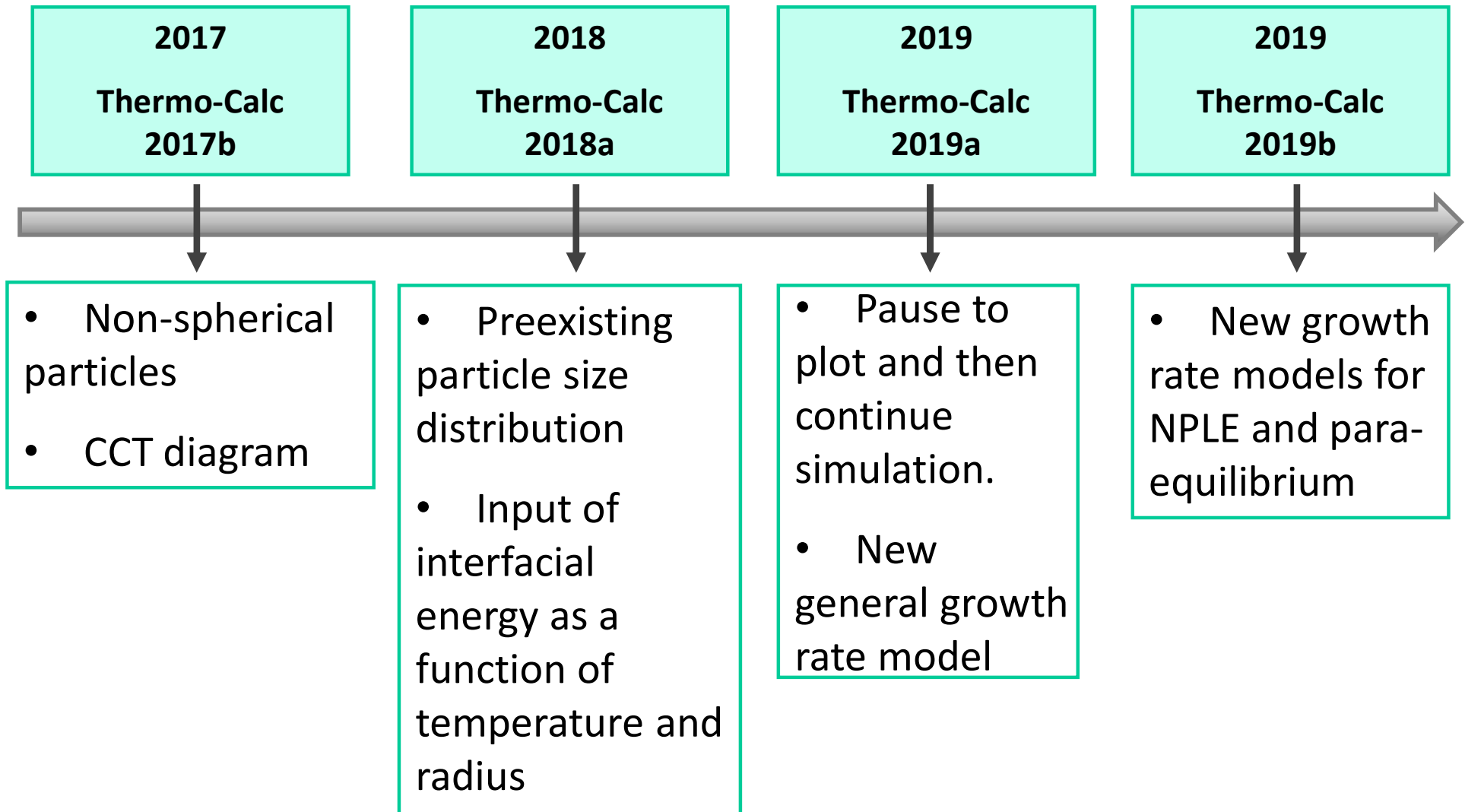
2016

Thermo-Calc
2016a

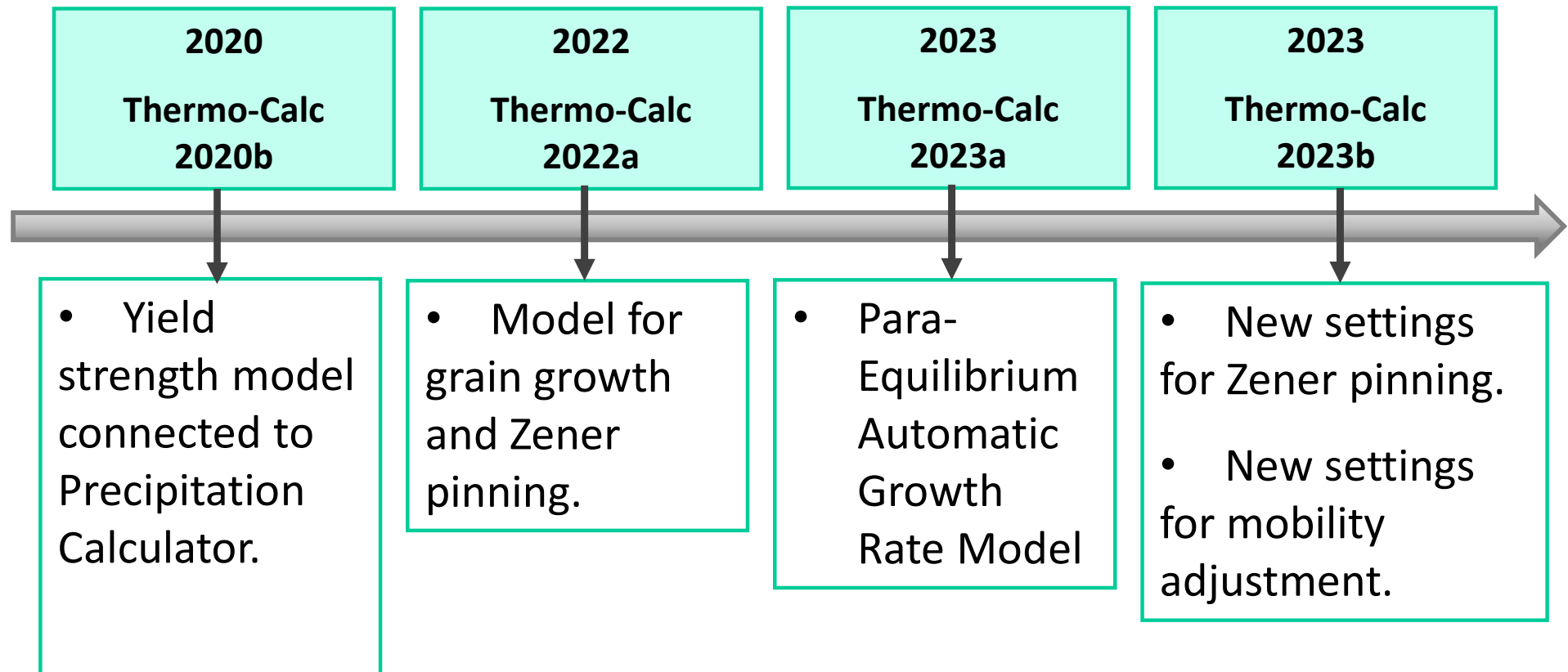
- Multiple Nucleation Types
- Wetting Angle for GB Precipitation
- Integration into Thermo-Calc
-



TC-PRISMA



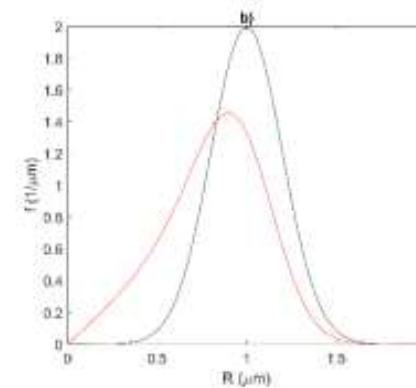
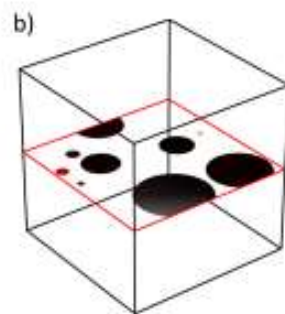
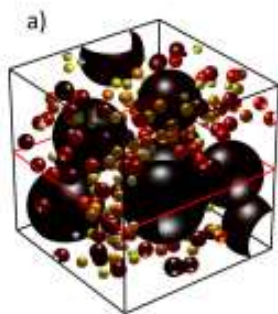
TC-PRISMA



2024

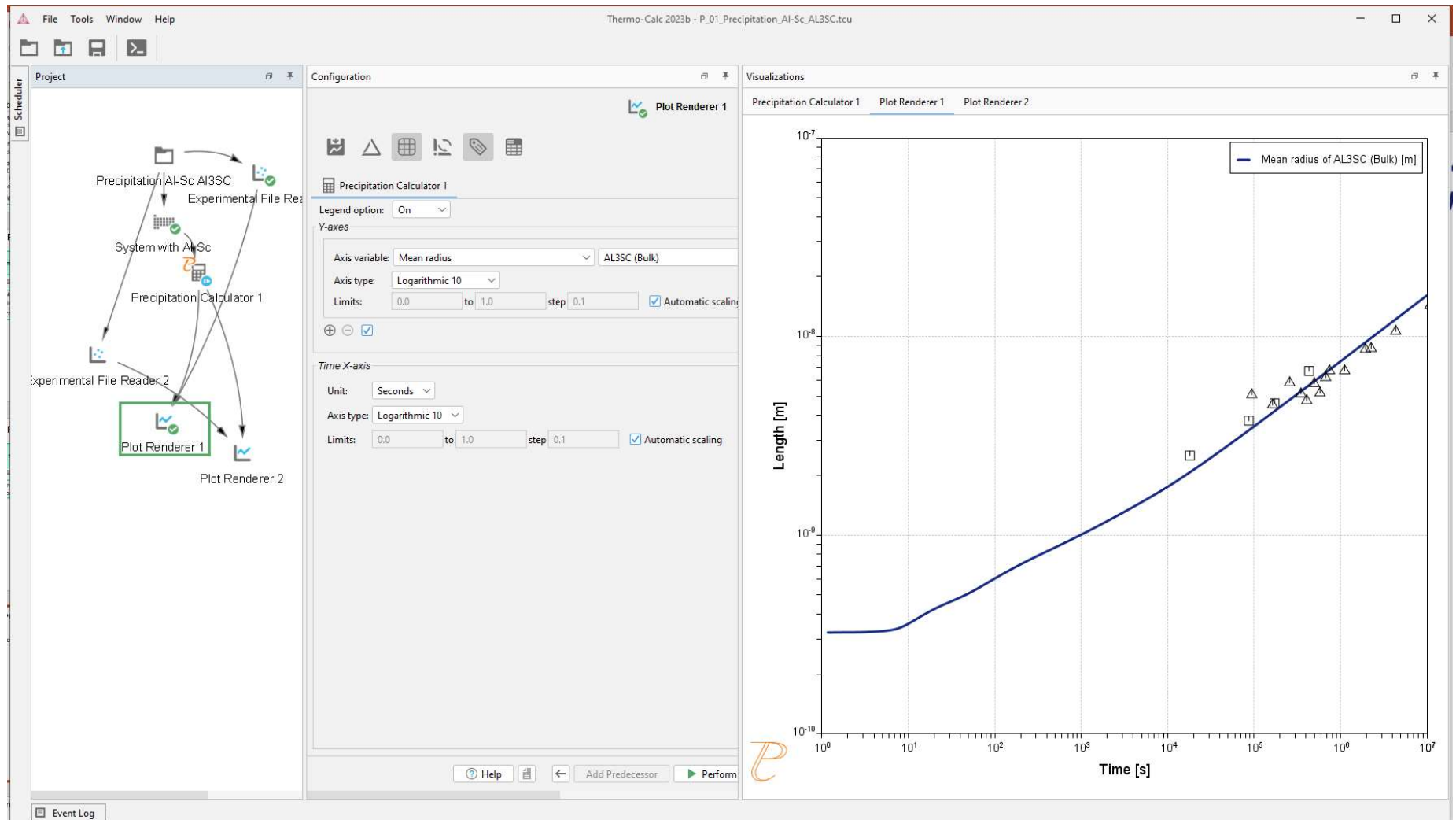
New in Thermo-Calc 2024a

- Transforming 3D size distribution to 2D. New Example P16.



- More options for entering existing Particle size distributions.
- Bug fixes.

Now formally known as Precipitation Simulation Module



Introduction – TC-PRISMA



Features:

- Concurrent nucleation, growth, and coarsening
- Multicomponent nucleation and growth models
- Account for different type of nucleation sites
- Treat cross diffusion and high supersaturation
- Estimation of multicomponent interfacial energy
- Non-spherical particles
- Para-equilibrium

- Integrated within Thermo-Calc
- Highly intuitive Graphic User Interface (GUI)
- Powered by Thermo-Calc and DICTRA calculation engine
- Linked to Thermo-Calc and DICTRA databases

TC-PRISMA vs DICTRA

DICTRA is for simulation of **D**iffusion **C**ontrolled **TR**ansformation in multicomponent system

- Single-phase problems: homogenization, carburization
- Moving boundary problems: solidification, dissolution, growth, and coarsening
- No nucleation, and no unified treatment to growth and coarsening
- For precipitation, good for detailed multicomponent analysis of composition profile evolution in diffusion zone

TC-PRISMA is for precipitation simulation with **multi-particle** interaction in multicomponent systems

- Unified treatment of nucleation, growth, dissolution, and coarsening of dispersed particles
- Not suitable for formation of non-dispersed high volume new phases

Introduction – TC-PRISMA

Input

- Thermodynamic data
- Kinetic data
- Alloy composition
- Temperature - Time
- Simulation time
- Property data
(Interfacial energy, volume, etc.)
- Nucleation sites and related microstructure information

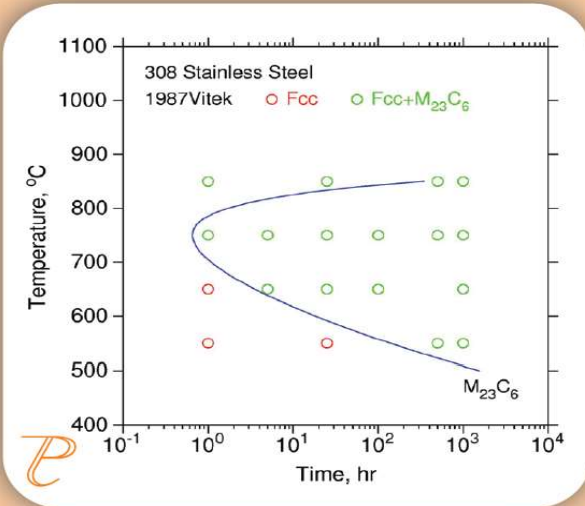
TC-PRISMA

Output

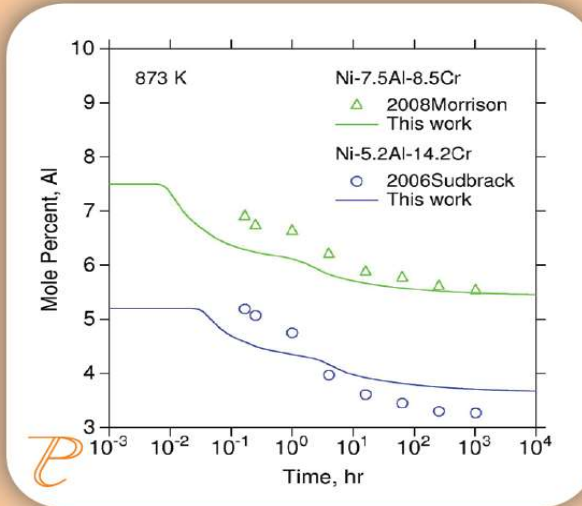
- Particle Size Distribution
- Number Density
- Average Particle Radius
- Volume Fraction
- Matrix composition
- Nucleation rate
- Critical radius
- Driving force
- Mean aspect ratio
- Aspect ratio distribution
- TTP/CCT diagrams
- Yield strength
- Grain size distribution

Introduction – TC-PRISMA

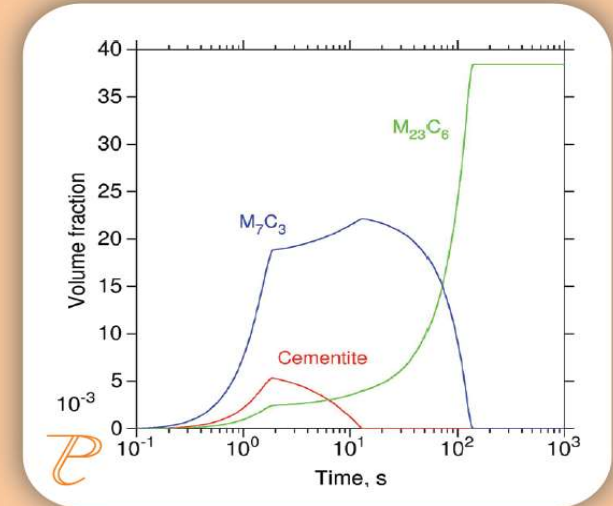
Example of results



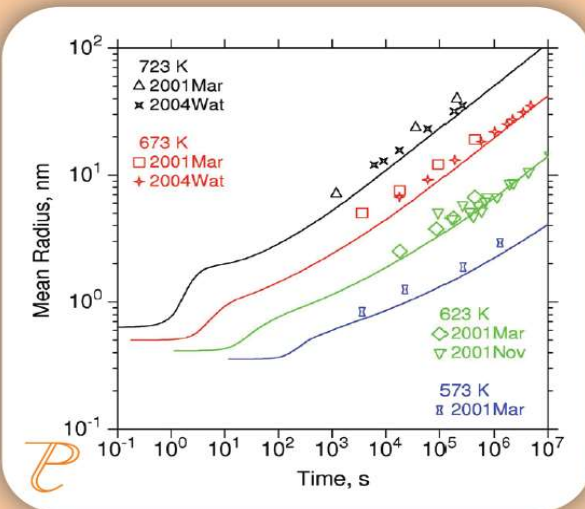
Time temperature precipitation of $M_{23}C_6$ in 308 stainless



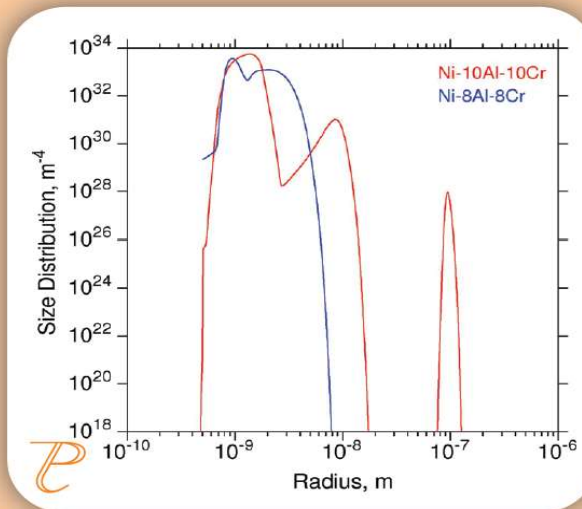
Average matrix composition vs time during precipitation



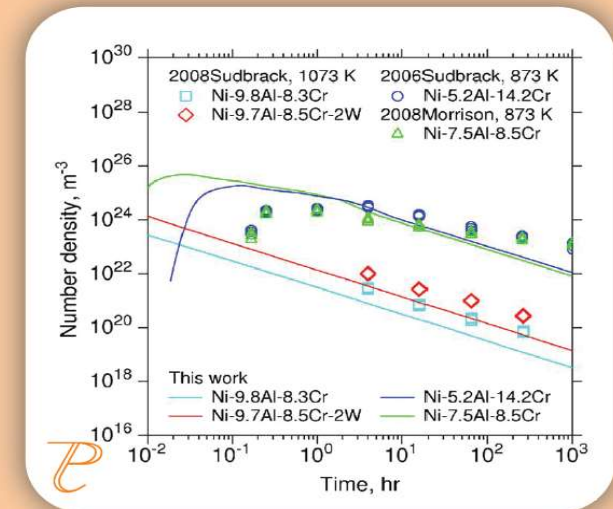
Precipitation of stable/metastable carbides in 12Cr steels



Mean radius of Al_3Sc precipitates vs time at various temperatures



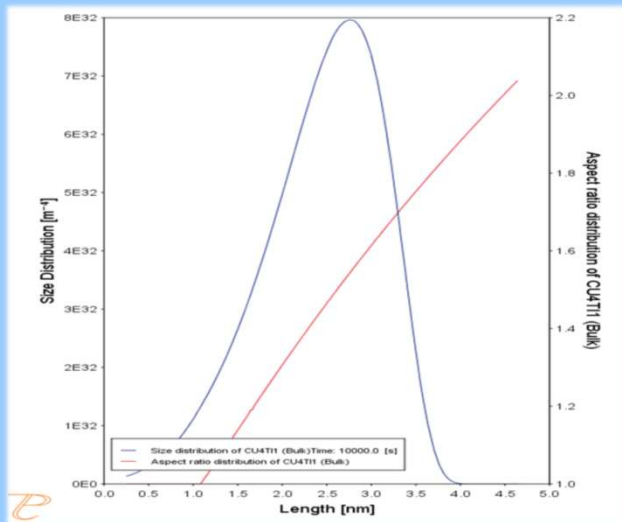
Multimodal size distribution of γ' during non-isothermal treatment



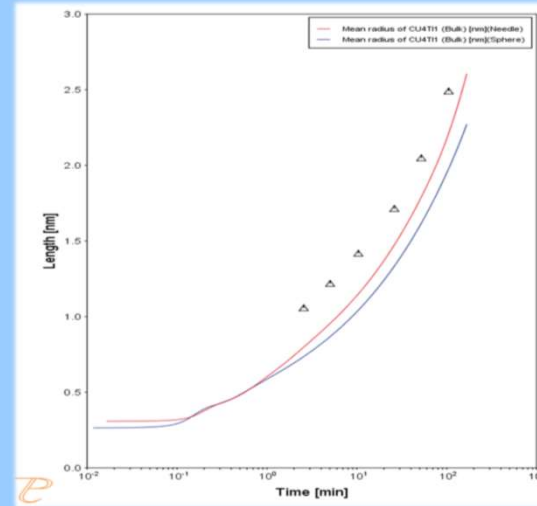
Number density of γ' vs time for various Ni-based superalloys

Introduction – TC-PRISMA

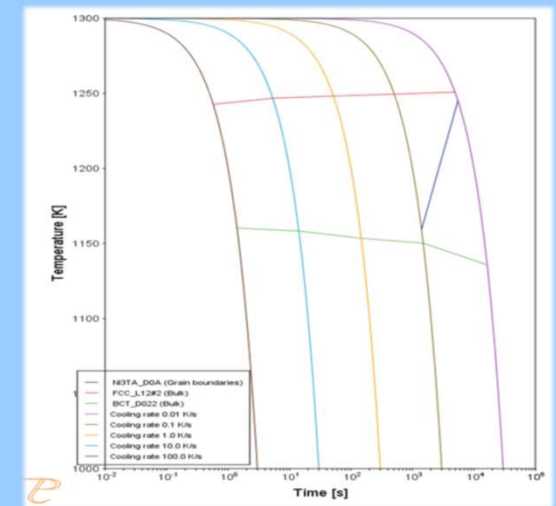
Example of results



Size distribution and Aspect ratio Distribution of Cu_4Ti needle-shaped particles

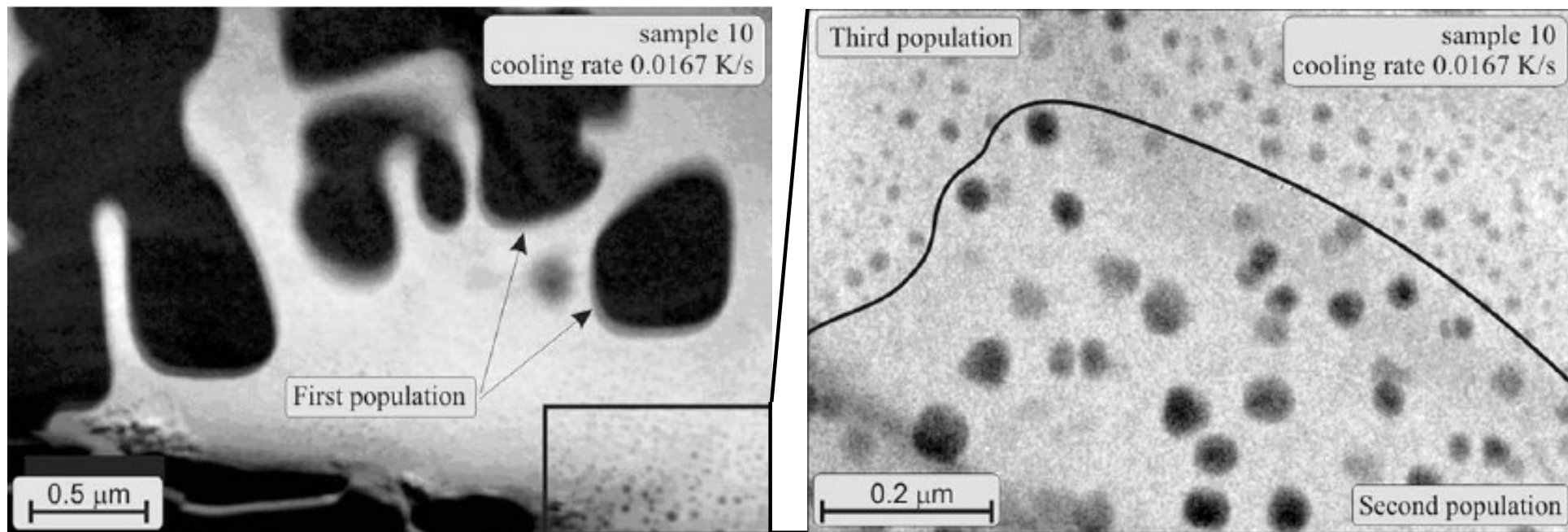


Size of Cu_4Ti needle- and sphere-shaped particles as a function of time



CCT curves from 0.01 K/s to 100 K/s for different precipitates in a Ni-superalloy

Non-Isothermal Conditions



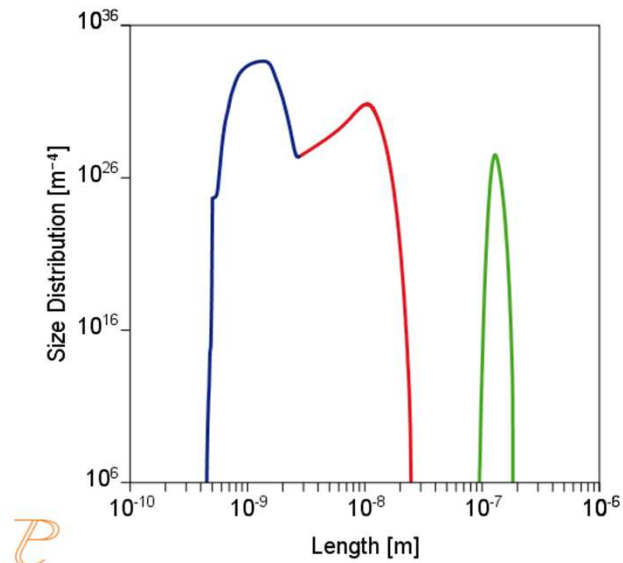
γ/γ' Microstructure in U720 Li

- Continuous cooling at 0.0167 K/s

Introduction – TC-PRISMA

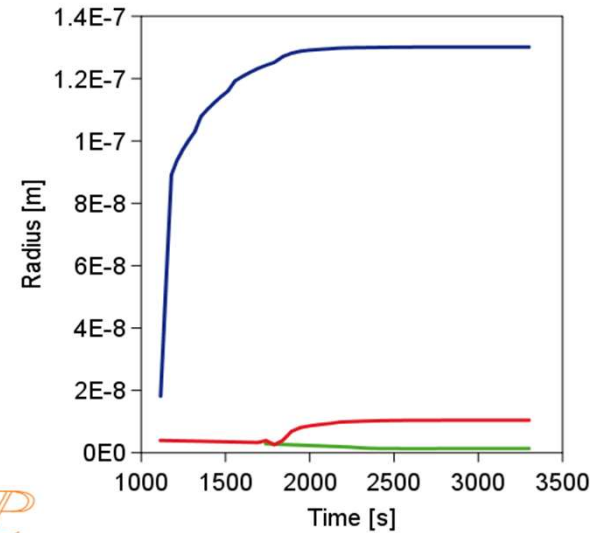
Multi-modal Distribution

Particle Size Distribution



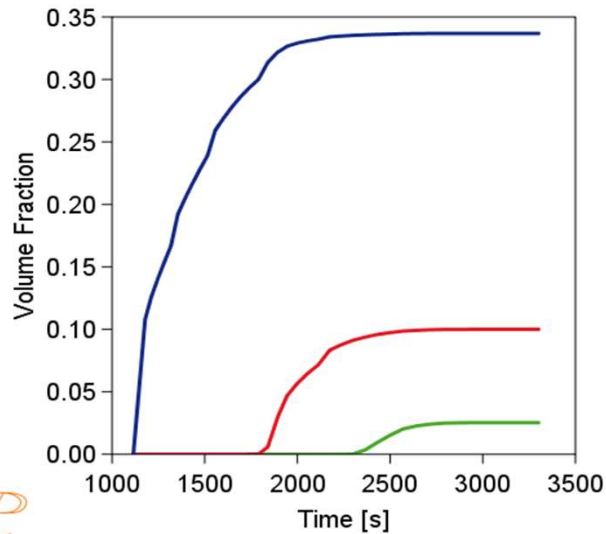
P

Mean Particle Size



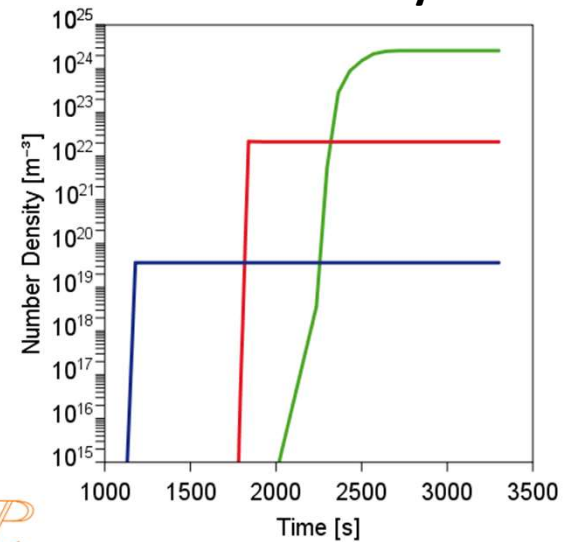
P

Volume Fraction



P

Number Density



P

Compatibility of Databases



Thermodynamic Database	Kinetic Database
SSOL2, SSOL4, SSOL5, SSOL6, SSOL7, SSOL8	MOB2
TCFE5 and earlier versions	MOB2
TCHEA2, TCHEA3+4+5, TCHEA6+7	MOBHEA1, MOBHEA2, MOBHEA3
TCFE6, 7, 8, TCFE9, TCFE10, TCFE11, TCFE12, TCFE13	MOBFE1, 2, 3, 4, 5, 6, 7, MOBFE8
TTNI8 and earlier versions	MOBNI1
TCNI4, TCNI5, TCNI6*	MOBNI2*
TCNI7, TCNI8	MOBNI3, MOBNI4
TCNI9+TCNI10+TCNI11, TCNI12	MOBNI5, MOBNI6
TTAL8 and earlier versions	MOBAL1 and BISHOP
TCTI4, TCTI5	MOBTI4
TCAL1+2+3, TCAL4,TCAL5, TCAL6+7, TCAL8, TCAL9	MOBAL3,4,5, MOBAL6, MOBAL7, MOBAL8
TCMG1+2+3+TCMG4+TCMG5, TCMG6	MOBMG1, MOBMG2
TCCU1, TCCU2, TCCU3, TCCU4, TCCU5 + TCCU6	MOBCU1, 2, 3, 4, MOBCU5

* Pairing of TCNI6 and MOBNI2 is not possible for LIQUID phase.

TC-PRISMA Software Basics

Simulation – Setup



System

- ^ Databases
- ^ Matrix/Precipitate phases



Conditions

- ^ Composition
- ^ Type of simulation
- ^ Thermal Profile
- ^ Nucleation Sites



Additional Data

- ^ Interfacial Energies
- ^ Phase Boundary Mobility
- ^ Phase Energy Additions
- ^ Mobility Enhancement
- ^ Phase Molar Volumes
- ^ Wetting angle
- ^ Grain size/ shape
- ^ Dislocation density
- ^ Elastic Properties
- ^ Particle Morphology
- ^ Existing size distribution

Calculation Settings

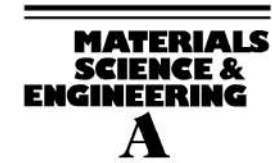
- ^ Numerical parameters
- ^ Growth Rate Model

Examples

Al Alloys



Materials Science and Engineering A318 (2001) 144–154



www.elsevier.com/locate/msea

Precipitation of Al₃Sc in binary Al–Sc alloys

Gabriel M. Novotny¹, Alan J. Ardell*

*Department of Materials Science and Engineering, School of Engineering and Applied Science, University of California, 405 Hilgard Avenue,
6531 Boelter Hall, Los Angeles, CA 90095, USA*

Received 21 September 2000; received in revised form 5 March 2001

Abstract

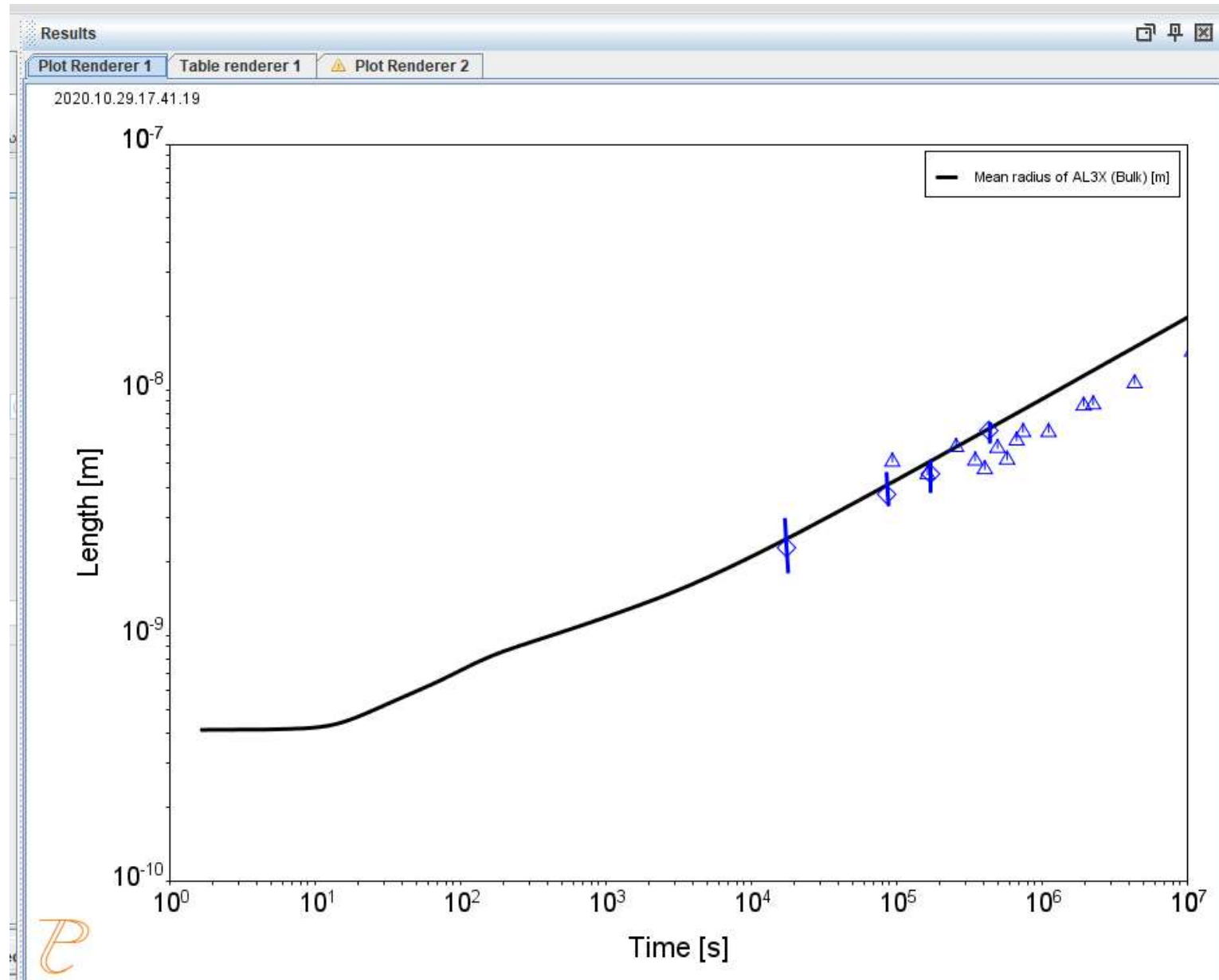
The precipitation of coherent Al₃Sc particles in Al–Sc alloys containing 0.06, 0.12 and 0.18 at.% Sc was investigated. The alloys were aged at 350°C for times up to 4663 h and the kinetics of particle growth, the particle size distributions and the evolution of particle morphology were measured and evaluated using transmission electron microscopy. Al₃Sc precipitates did not nucleate homogeneously in the most dilute alloy; this result was unexpected because 0.06 at.% Sc exceeds the solubility limit at 350°C. Persistent dislocation networks were observed in the alloy containing 0.12 at.% Sc under normal solution treatment conditions (e.g. 1 h at 600°C) and the dislocations acted as heterogeneous nucleation sites. The dislocations were ultimately eliminated using a very long solution treatment time of ~70 h near the melting temperature. Aging of both of the more concentrated alloys produced coherent precipitates. At short aging times the particles in the alloy containing 0.12% Sc were cauliflower-shaped and became spherical at longer times. At 4663 h some of the precipitates in this alloy were cuboidal, while others appear to have become semicoherent. The precipitates in this alloy were highly resistant to coarsening, and their size distributions were for the most part narrower than that predicted by the classical theory of Lifshitz, Slezov and Wagner (the LSW theory). The shapes of the precipitates in the alloy containing 0.18% Sc evolved from spherical to cuboidal with increasing aging time. The kinetics of growth of the precipitates in this alloy were consistent with the predictions of the LSW theory, the average size, $\langle r \rangle$, increasing with aging time, t , according to an equation of the type $\langle r \rangle^3 \simeq kt$. The experimentally measured rate constant, k , was in very good agreement with that calculated theoretically for this alloy. © 2001 Elsevier Science B.V. All rights reserved.

Keywords: Al–Sc; Precipitation; Coarsening; Microstructure; Kinetics

Example 1: Al - Sc Alloy

System	
Database package	TCAL9 + MOBAL7
Elements	Al, Sc
Matrix phase	Fcc_A1
Precipitate phase	Al ₃ Sc (= AL3X in database)
Conditions	
Composition	Al - 0.18 Sc (at.%)
Temperature	350 °C
Simulation time	1E7 s
Nucleation properties	Nucleation Site Type: Bulk
Data Parameters	
Interfacial Energy	Bulk: 0.074 J/m ²
Molar Volume (Matrix):	Fcc_A1: from database
Molar Volume (Precipitate):	Al ₃ Sc: from database

TC-PRISMA Example

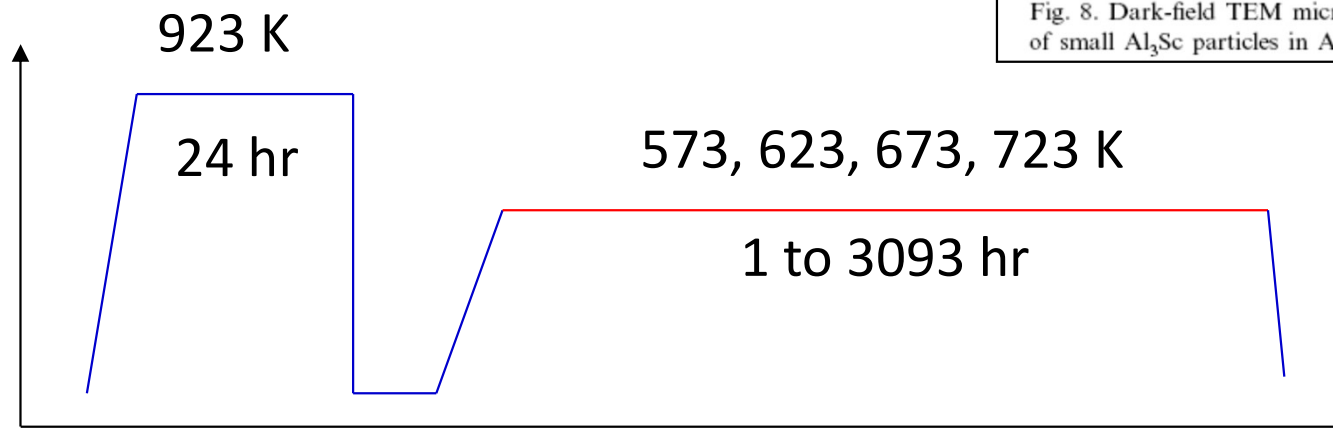
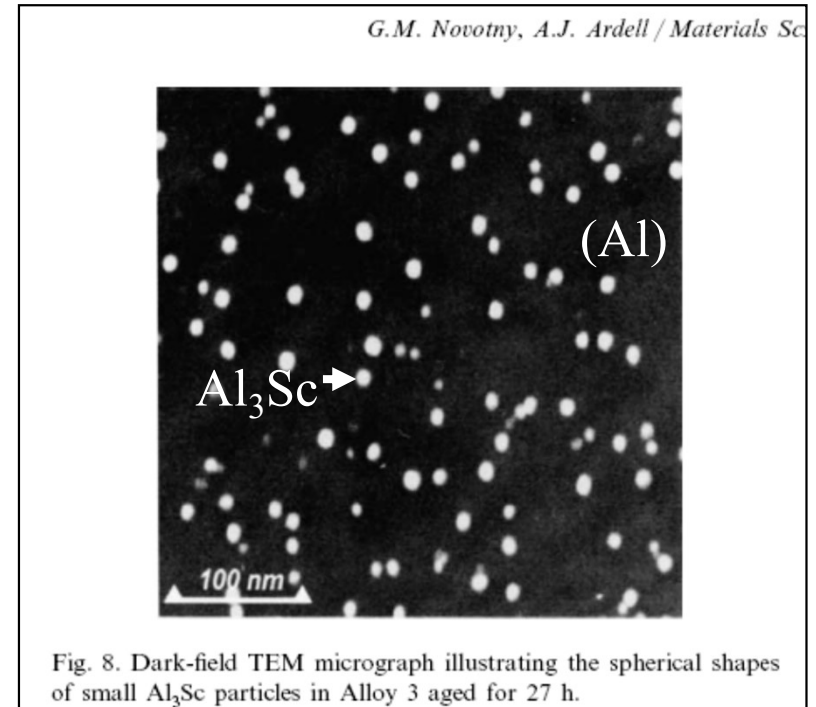


Application – Al-Sc Alloy

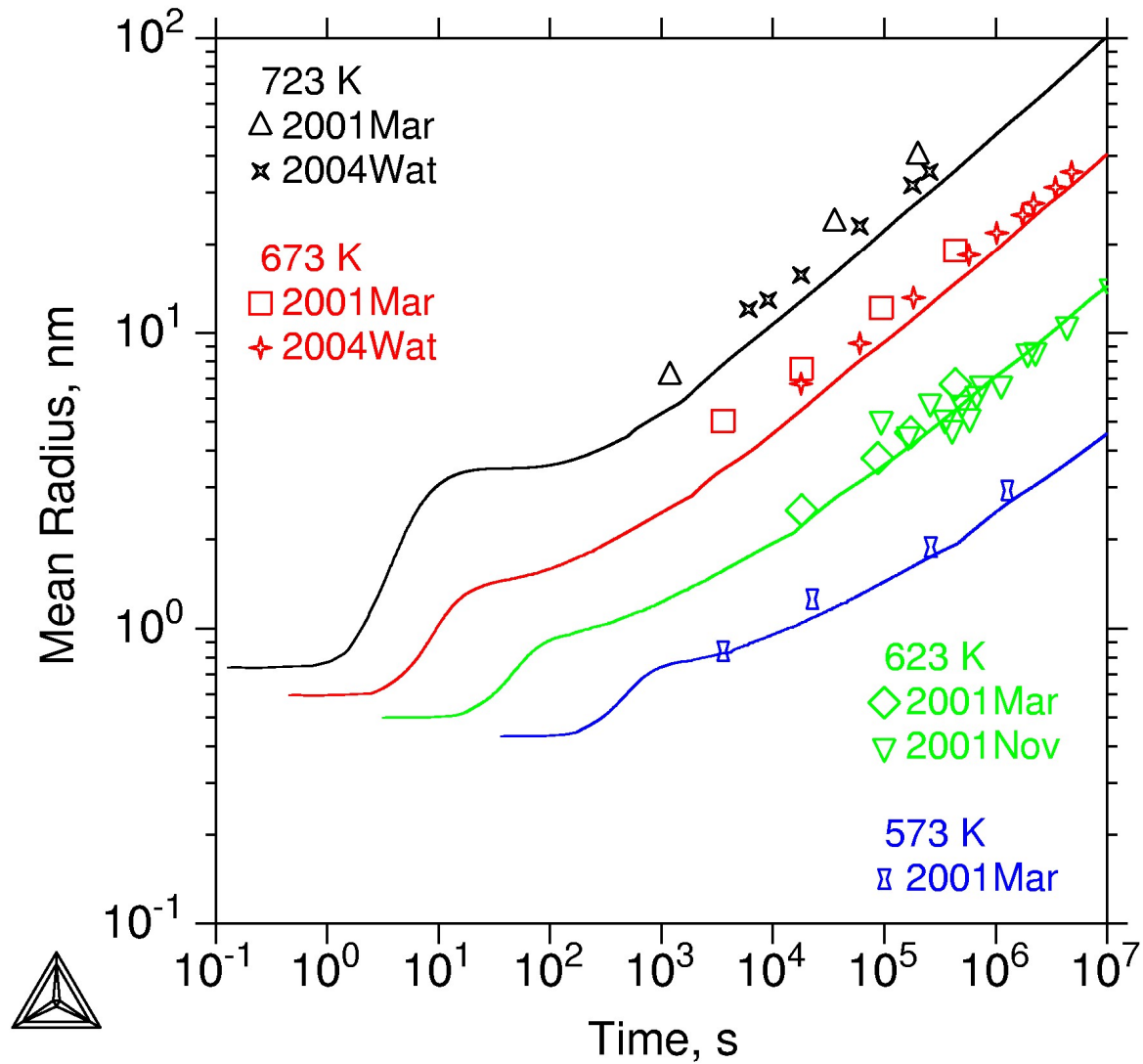
Novotny&Ardell, MSE, A318(2001)144; Marquis&Seidman, AM, 49(2001)1909;
Watanabe et al., MMT, 35A(2004)3003.

Al-0.18at%Sc and Al-0.17at%Sc

$$\sigma = 0.093 \text{ J/m}^2$$



Results – Al-Sc



Results – Al-Mg-Sc

Marquis & Seidman, Acta Mater. 53(2005)4259-4268.

Al-2.2at%Mg-0.12at%Sc

$$\sigma = 0.093 \text{ J/m}^2$$

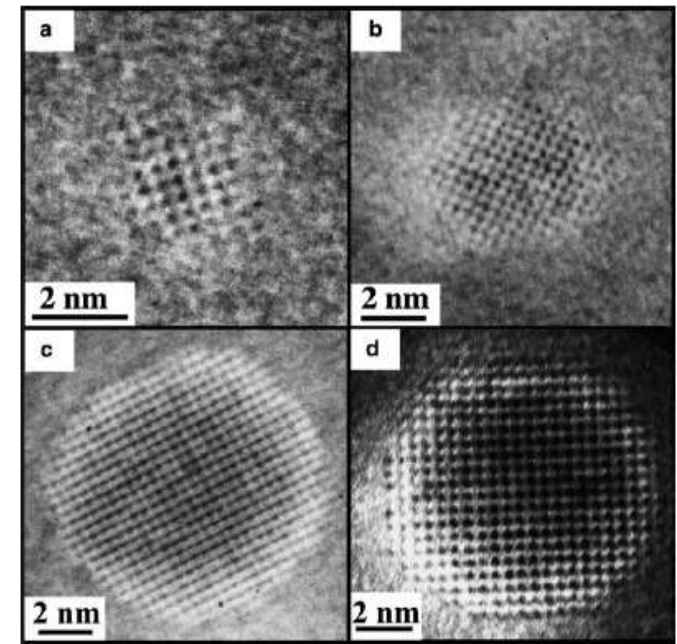
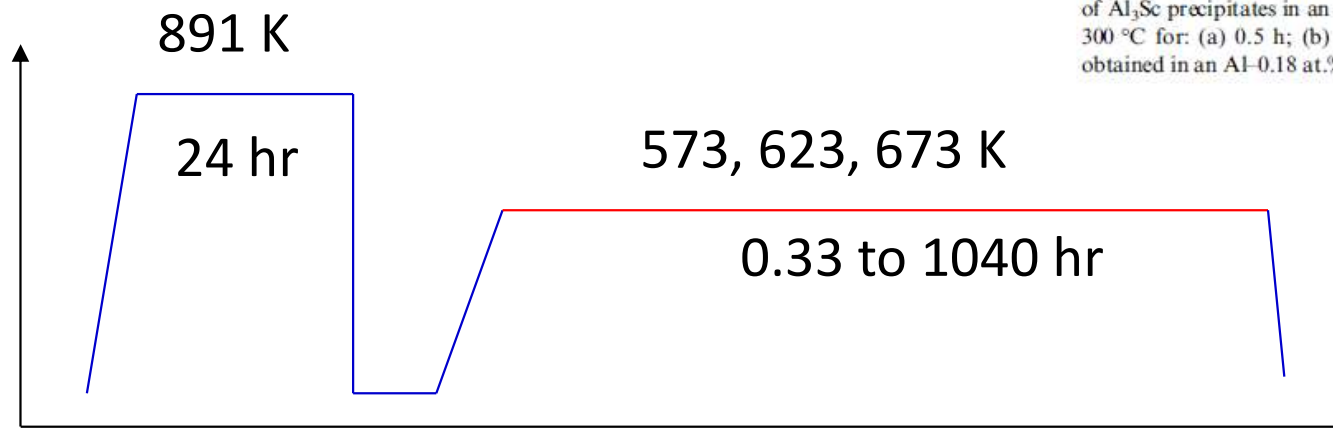
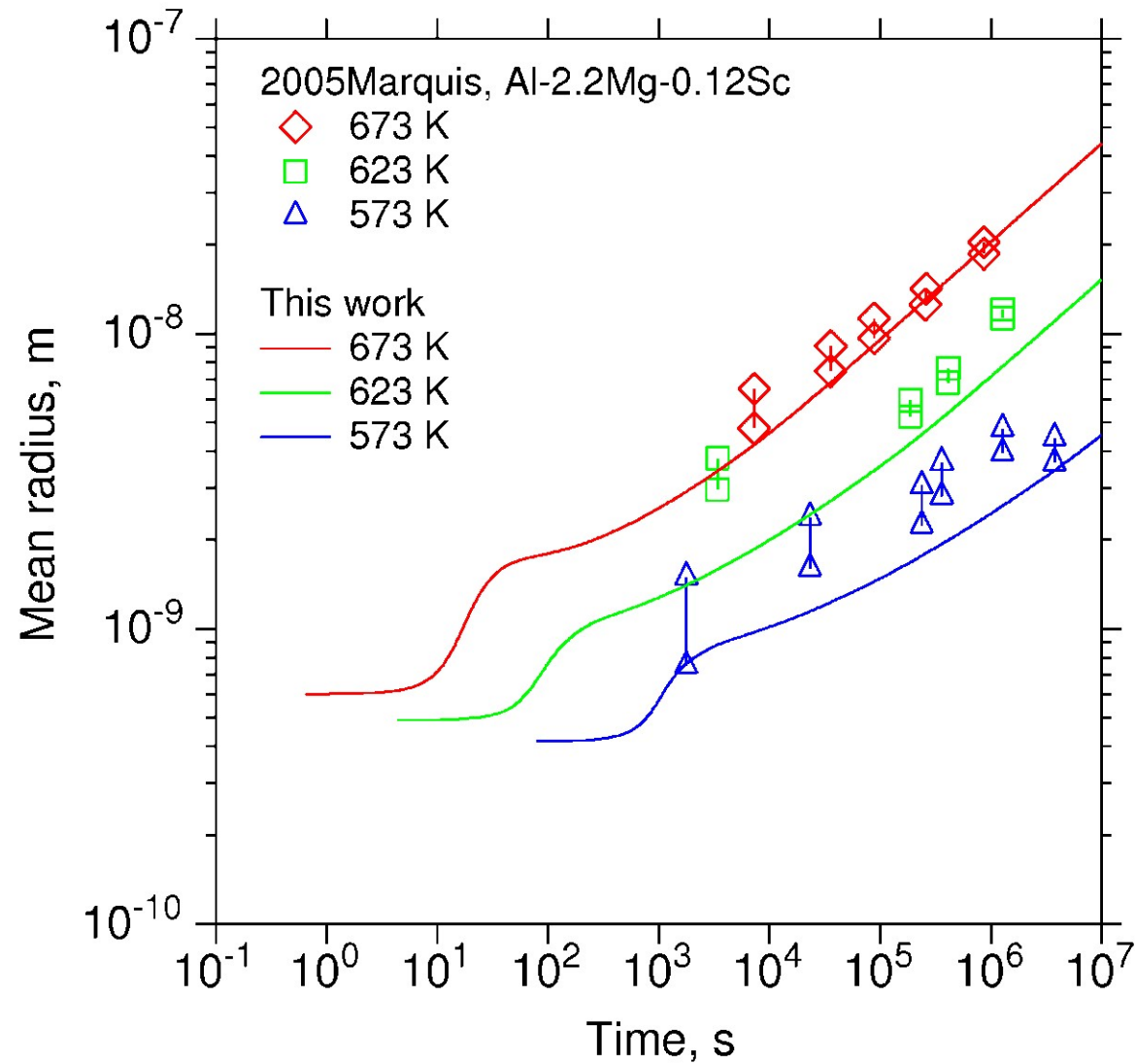


Fig. 3. High-resolution electron microscope images ([100] zone axis) of Al_3Sc precipitates in an Al-2.2 Mg-0.12 Sc at.% alloy after aging at 300 °C for: (a) 0.5 h; (b) 5 h; (c) 1040 h; and (d) Al_3Sc precipitate obtained in an Al-0.18 at.% Sc alloy after aging at 300 °C for 350 h [3].



Results – Al-Mg-Sc

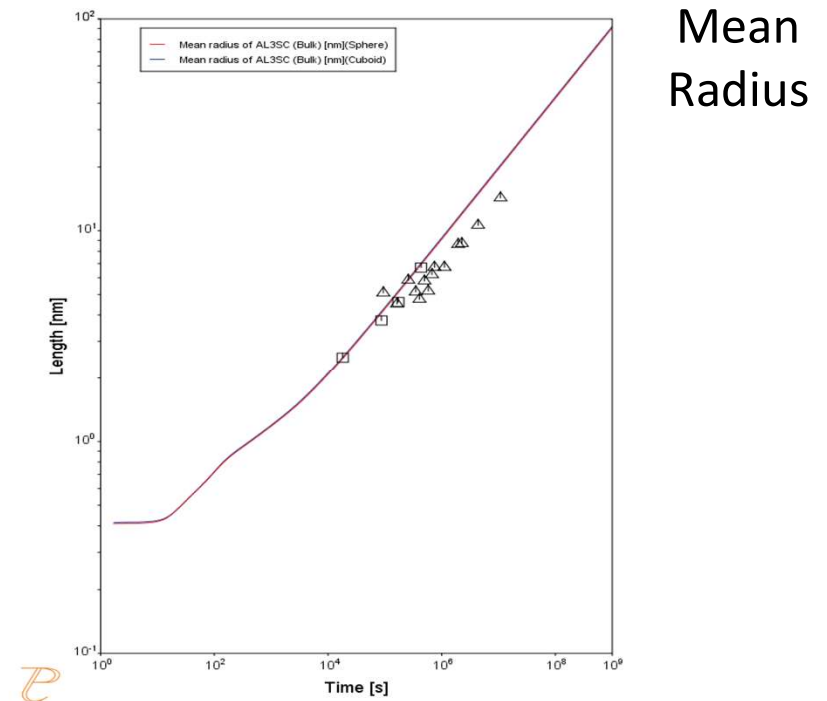
Same set of physical parameters as binary Al-Sc.



Example 2: Al-Sc Alloy

Precipitation of Al₃Sc from FCC

- Al-0.18at.% Sc
- Databases:
TCAL9+MOBAL7
- Misfit strain calculated from molar volume
- Default values for other parameters
- User defined interfacial energy:
0.074 J/m²
- T = 350°C for 1E9s

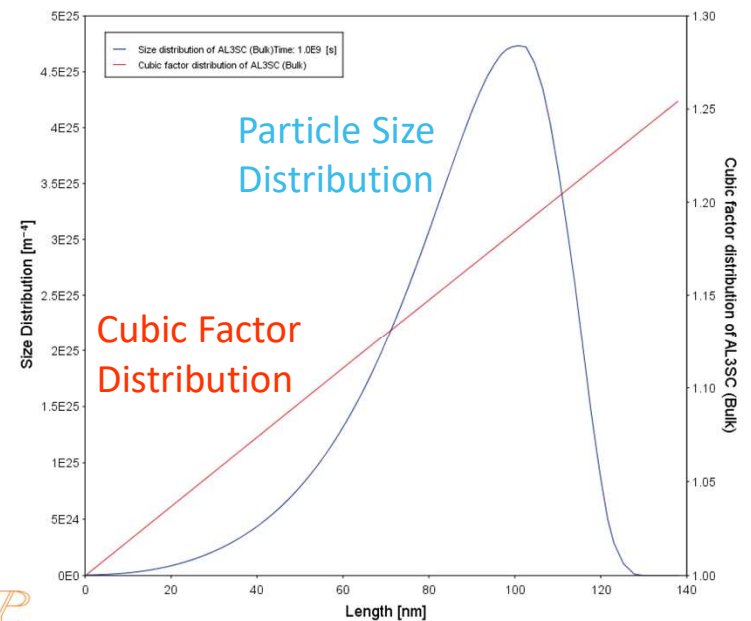
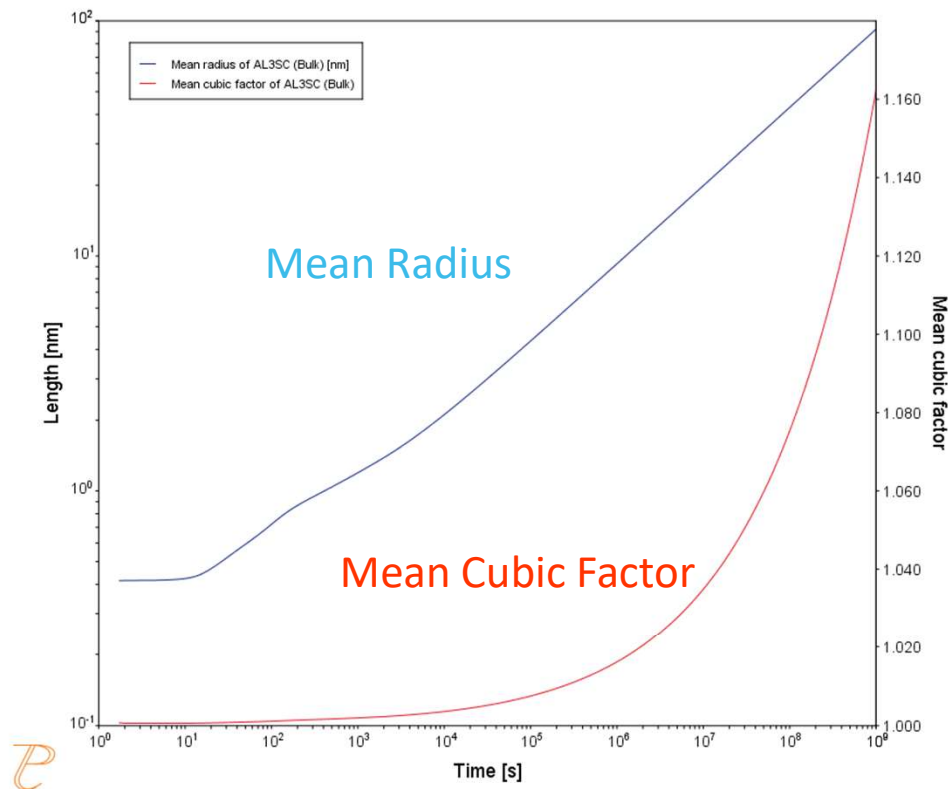


C_{11}	C_{12}	C_{44}
108.2 GPa	61.3 GPa	28.5 GPa

* J.K. Lee et al., Metall. Trans. A, 8(1977)963

Example: Al-Sc Alloy

- Spherical to Cubic Shape with Increasing Particle Size



* TEM picture from G.M. Novotny and A.J. Ardell, *Mater. Sci. Eng.* A318(2001)144



Available online at www.sciencedirect.com

SCIENCE @ DIRECT®

Acta Materialia 52 (2004) 591–600



www.actamat-journals.com

Loss in coherency and coarsening behavior of Al₃Sc precipitates

S. Iwamura *, Y. Miura

*Department of Materials Physics and Chemistry, Graduate School of Engineering, Kyushu University,
6-10-1 Hakozaki, Higashi-ku, Fukuoka 812-8581, Japan*

Received 18 August 2003; received in revised form 18 August 2003; accepted 29 September 2003

Abstract

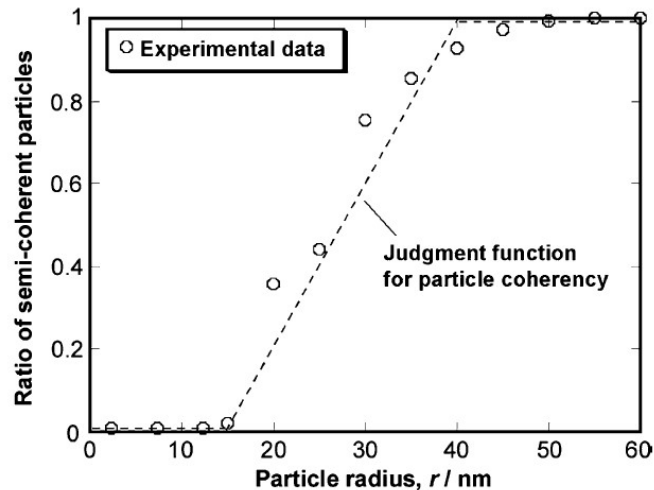
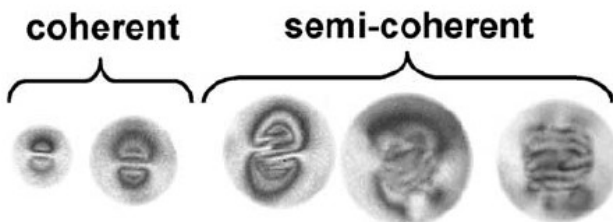
The coarsening behavior of the Al₃Sc particles in Al–0.2wt%Sc alloy at 673–763 K is studied on the basis of TEM observations with the numerical model. Emphasis is on the effects of coherent/semi-coherent transition of the particles. The radius for coherent/semi-coherent transition of the Al₃Sc particles is determined from TEM micrographs as 15–40 nm. The average particle radius, r_{ave} , of the Al₃Sc particles obeys the r_{ave}^3 growth law both in the coherent stage ($r_{\text{ave}} < 15$ nm) and semi-coherent stage ($r_{\text{ave}} > 40$ nm). However, in the intermediate stage, where coherent and semi-coherent particles coexist ($15 < r_{\text{ave}} < 40$ nm), coarsening is delayed and particle size distribution is broadened in the experiment and also in the calculation. These results are qualitatively understood in consideration of the different growth rates of individual particles in the intermediate stage.

© 2003 Acta Materialia Inc. Published by Elsevier Ltd. All rights reserved.

Example 3 – Al Alloys

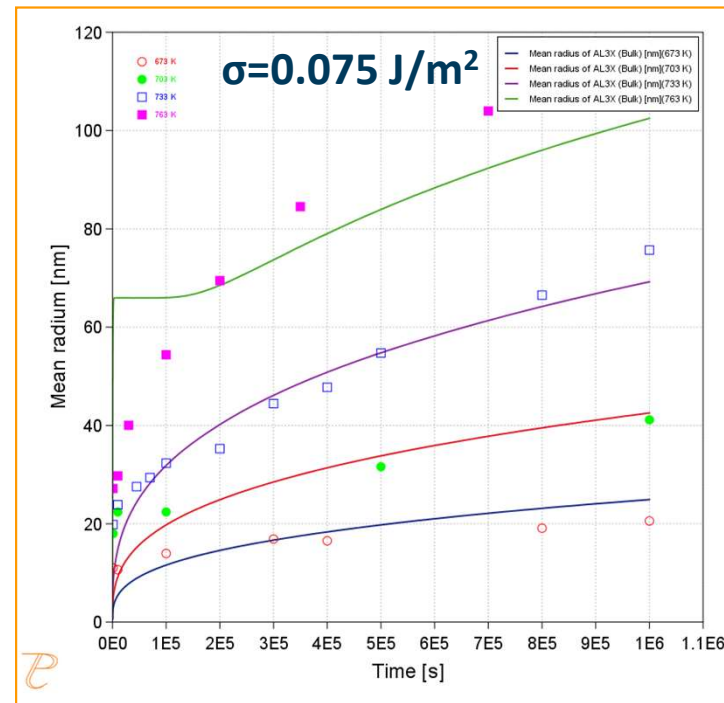
□ $\sigma=0.075 \text{ J/m}^2$ using
TCAL9 +MOBAL7

○ Al-0.12 at.% Sc, solution
treated at 640 °C for 2 h.



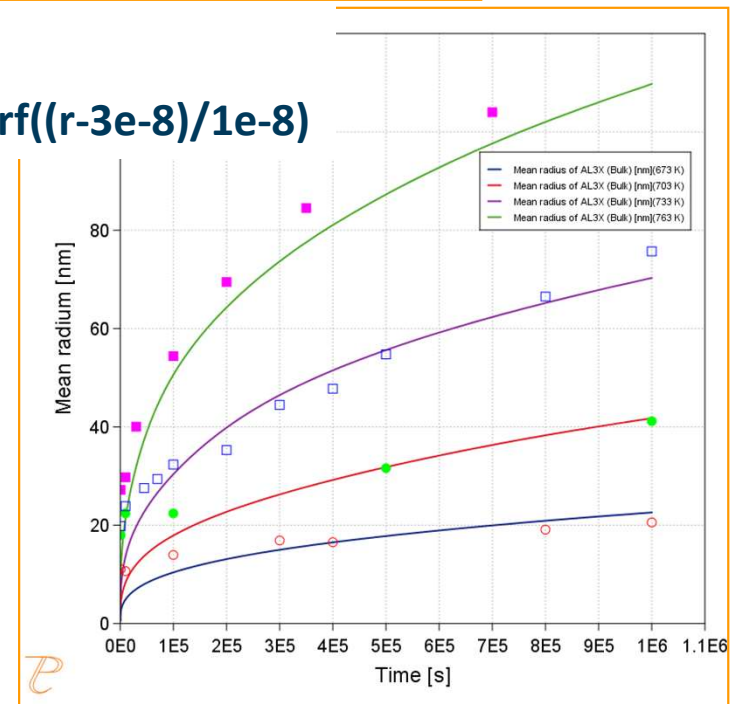
□ Size dependence of interfacial energy

- Due to coherency loss



Error function

$$\sigma=0.075+0.011*\text{erf}((r-3\text{e}-8)/1\text{e}-8)$$



Example 3: Al - Sc Alloy

System	
Database package	TCAL9 + MOBAL7
Elements	Al, Sc
Matrix phase	FCC_A1
Precipitate phase	Al ₃ Sc (= AL3X in database)
Conditions	
Composition	Al - 0.12 Sc (at.%)
Temperature	673, 703, 733 and 763 K
Simulation time	1E7 s
Nucleation properties	Nucleation Site Type: Bulk
Data Parameters	
Interfacial Energy	Bulk: $0.075 + 0.011 * \text{erf}((r - 3e-8)/1e-8)$
Molar Volume (Matrix):	Fcc_A1: from database
Molar Volume (Precipitate):	Al ₃ Sc: from database

Example 3 – Al Alloys

The error function, $\text{erf}(x)$, is used to input the size dependent interfacial energy in this example. Below is a diagram to remind us of its properties.

$\text{Erf}(x)$ can be used as a simple solution to binary diffusion problems, and can be used to smooth out step-like composition-input profiles in DICTRA. The sharpness of the the step-like profile can be set by the user.

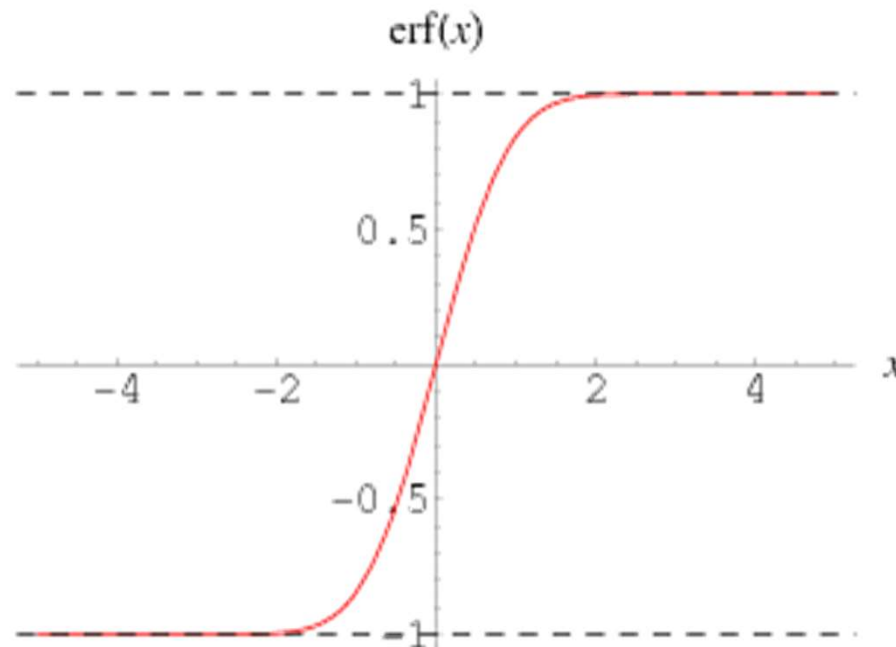


Image from:
<http://mathworld.wolfram.com/Erf.html>

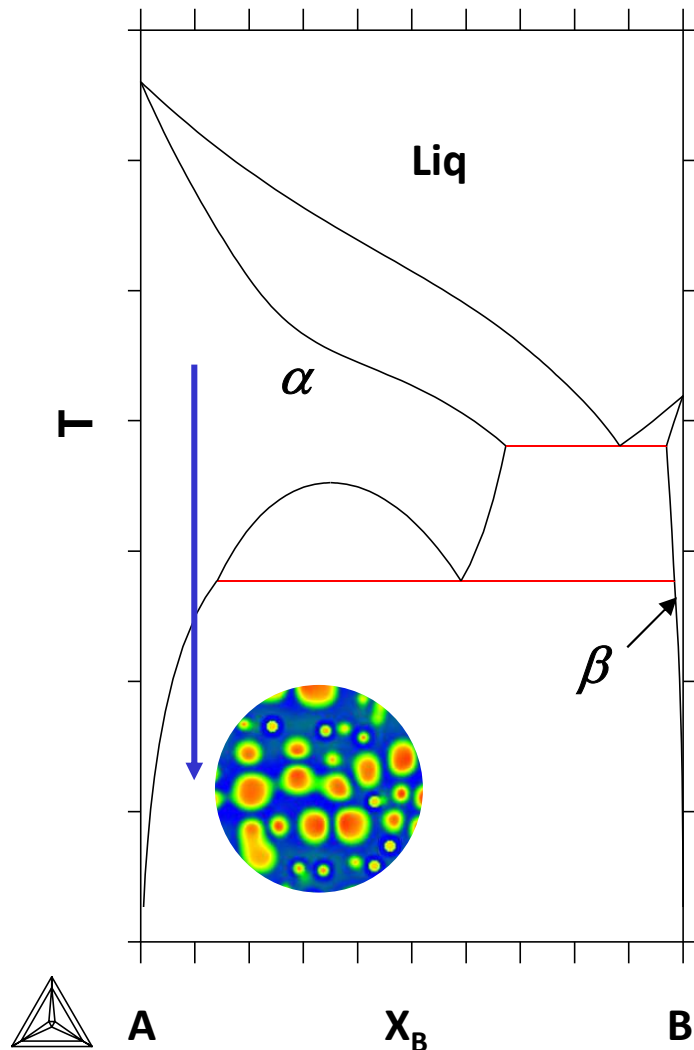
Q & A

Theory: Nucleation

Models and Model Parameters

LS (Langer-Schwartz) and KWN (Kampmann and Wagner Numerical) Approach

$$J = \int_{r^*}^{\infty} j(r) dr$$



Continuity equation

$$\frac{\partial f(r,t)}{\partial t} = - \frac{\partial}{\partial r} [v(r) f(r,t)] + j(r,t)$$

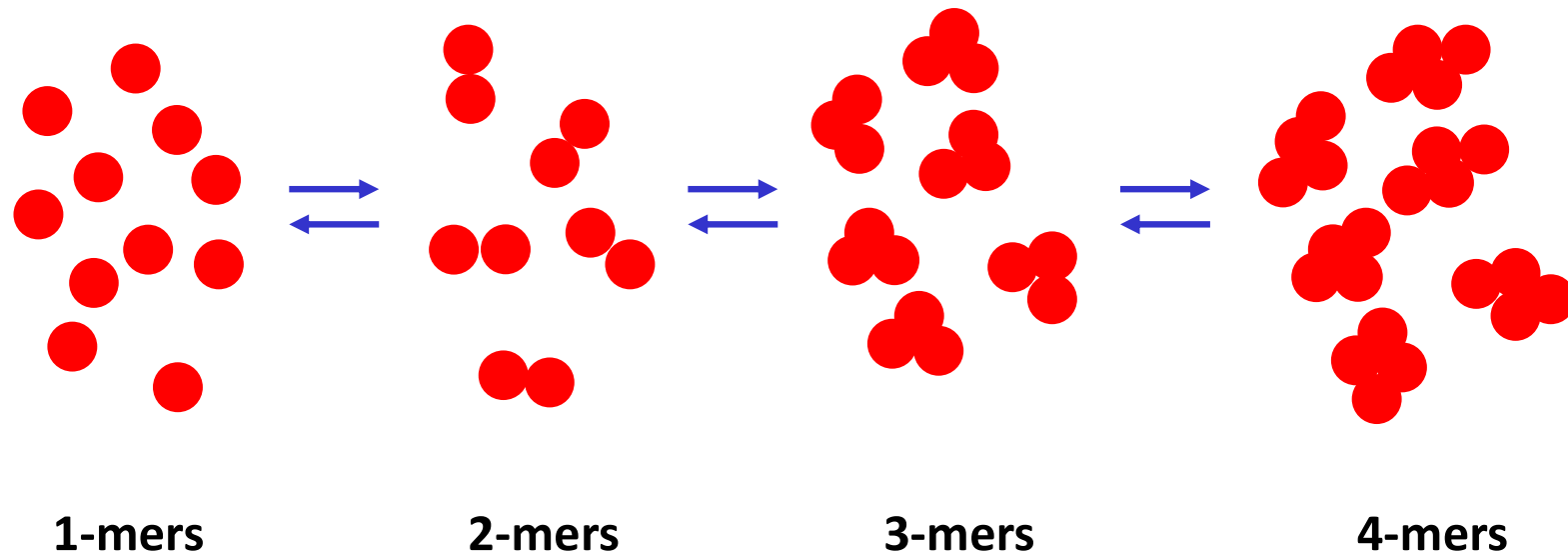
$$C_0^\alpha = C^\alpha + (C^\beta - C^\alpha) \int_0^\infty \frac{4\pi}{3} f(r,t) r^3 dr$$

Mass balance



Models: Nucleation Rate

Classic Nucleation Theory (CNT)



$$\frac{\partial N_{n,t}}{\partial t} = \frac{\partial}{\partial n} \left[\beta(n) \frac{\partial N_{n,t}}{\partial n} \right] + \frac{\partial}{\partial n} \left[N_{n,t} \frac{\beta(n)}{kT} \frac{\partial \Delta G_n}{\partial n} \right]$$

Zeldovich–Frenkel equation

Models: Nucleation Rate

Classical Nucleation Theory (CNT)

$$J(t) = J_s \exp\left(-\frac{\tau}{t}\right)$$

J: nucleation rate

J_s : steady state nucleation rate

τ : incubation time

$$J_s = Z\beta^* N \exp\left(\frac{-\Delta G^*}{kT}\right)$$

N: potential nucleation sites

Z: Zeldovich Factor

β^* : molecular attachment rate

$$\Delta G^* = \frac{16\pi\sigma^3 V_m^2}{3\Delta G_m^2}$$

σ : interfacial energy of matrix/precipitate

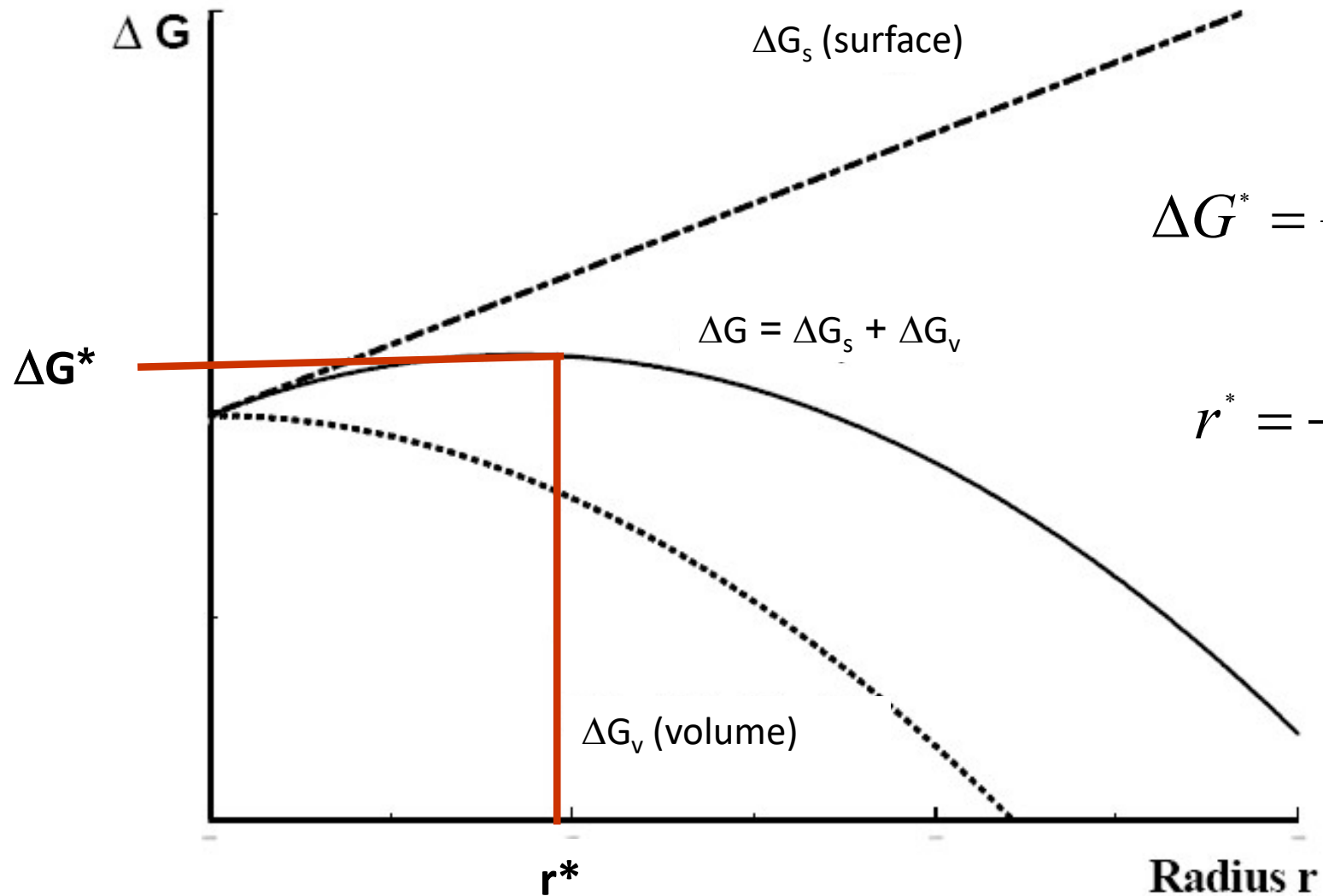
V_m : molar volume of precipitate phase

ΔG_m : driving force for nucleation

ΔG^* : energy barrier for nucleation

Models: Nucleation Rate

ΔG^* and r^*



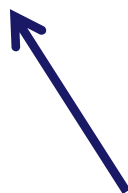
$$\Delta G^* = \frac{16\pi\sigma^3 V_m^2}{3\Delta G_m^2}$$

$$r^* = -\frac{2\sigma V_m}{\Delta G_m}$$

Models: Nucleation Rate

τ - incubation time

$$\tau = \frac{1}{\Theta Z^2 \beta^*}$$

$$\tau = \frac{1}{2Z^2 \beta^*}$$
A blue arrow points from the bottom left towards the coefficient '2' in the denominator of the equation.

Θ : constant (depending on assumptions/model derivation)

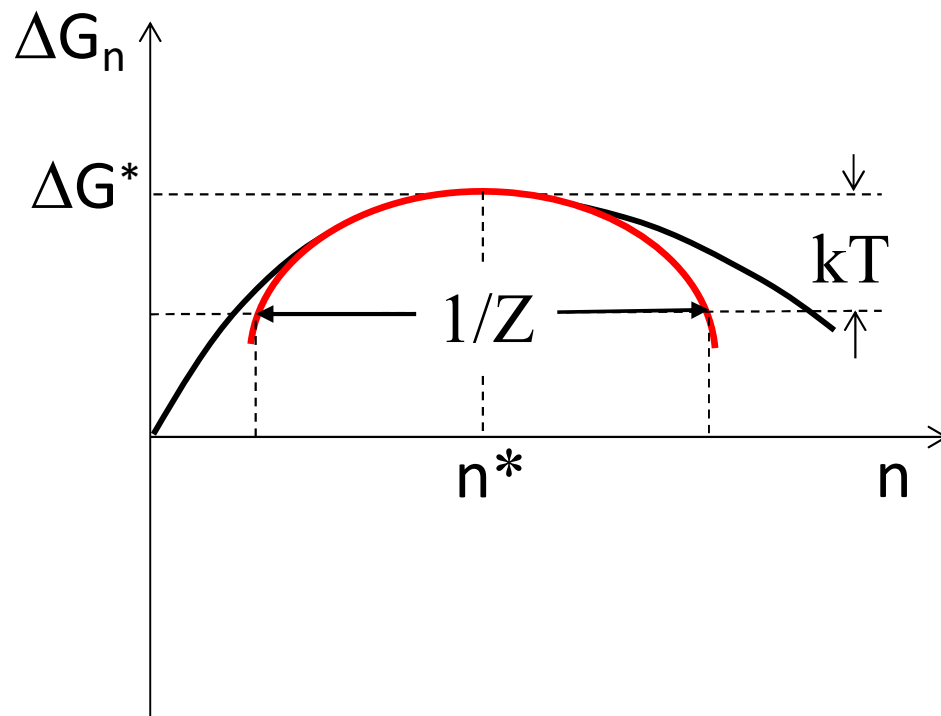
Z: Zeldovich Factor

β^* : attachment kinetics

- used in TC-PRISMA
- based on : Feder et al.; Advances in Physics 15 (1966)111-178

Models: Nucleation Rate

Zeldovich factor (thermodynamic):
accounts for deviation of steady-state concentration of critical nuclei with size n^* from equilibrium concentration



$$Z = \left\{ \frac{-1}{2\pi kT} \left(\frac{\partial^2 \Delta G_n}{\partial n^2} \right)_{n^*} \right\}^{1/2}$$

- Corresponds to curvature of ΔG_n
- Higher curvature leads to higher probability for super-critical nuclei to survive

Models: Nucleation Rate

β^* - molecular attachment rate

$$\beta^* = \frac{4\pi r^{*2} XD}{a^4} \quad \text{binary}$$

$$\beta^* = \frac{4\pi r^{*2}}{a^4} \left[\sum_{i=1}^n \frac{(X_i^{\beta/\alpha} - X_i^{\alpha/\beta})^2}{X_i^{\alpha/\beta} D_i} \right]^{-1}$$

$4\pi r^{*2}$: surface of critical nucleus

a : lattice spacing

D_i : diffusion constants in matrix

Svoboda J, Fischer FD, Fratzl P, Kozeschnik E. Materials science and engineering a 2004;385:166-174.

Models: Nucleation Rate

Classic Nucleation Theory (CNT)

From grain size, dislocation density, etc

$$J(t) = J_s \exp\left(-\frac{\tau}{t}\right) \quad J_s = Z\beta^* N \exp\left(\frac{-\Delta G^*}{kT}\right)$$

$$Z = \frac{V_m^\beta}{2\pi N_A r^{*2}} \sqrt{\frac{\sigma}{kT}} \quad \beta^* = \frac{4\pi r^{*2}}{a^4} \left[\sum_{i=1}^n \frac{(X_i^{\beta/\alpha} - X_i^{\alpha/\beta})^2}{X_i^{\alpha/\beta} D_i} \right]^{-1}$$

Interfacial energy, Volume

2004Svoboda

$$r^* = -\frac{2\sigma V_m^\beta}{\Delta G_m^{\alpha \rightarrow \beta}} \quad \Delta G^* = \frac{16\pi\sigma^3 V_m^2}{3\Delta G_m^2} \quad \tau = \frac{1}{2Z^2 \beta^*}$$

Models: Nucleation Rate

ΔG_m : driving force for nucleation

Nuclear Composition—A Factor of Interest in Nucleation*

Nucleation in the solid state is a very complicated process. Therefore, theoretical investigations in this field deal with simplified models. Some factors are examined while other factors are neglected. A factor that is usually neglected is the uncertainty of the nucleus composition. It is not necessarily true that the nuclei which form most readily have the composition appropriate for the precipitate, when equilibrium has been established. In the present note this point will be examined, on the assumption that many other factors can be neglected.

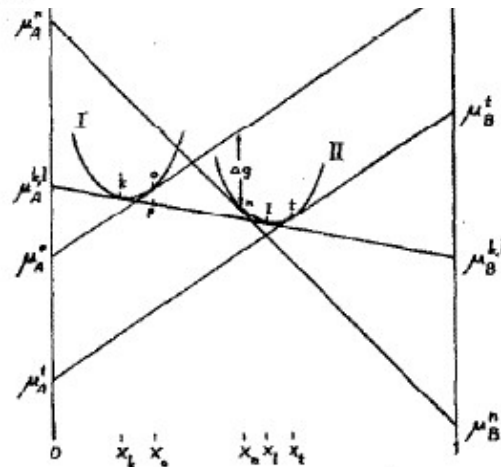


FIGURE 1. Free-energy diagram. The point *o* represents the parent phase. x_t is the thermodynamically most favourable nuclear composition.

MATS HILLERT

Metallografiska Institutet
Stockholm, Sweden

764 ACTA METALLURGICA, VOL. 1, 1953

tension the nucleus should exhibit a composition between that of the parent phase and that of the equilibrium precipitate. In the present paper a thermodynamic treatment will be carried out under the assumption that the surface tension of the nuclei is independent of composition.

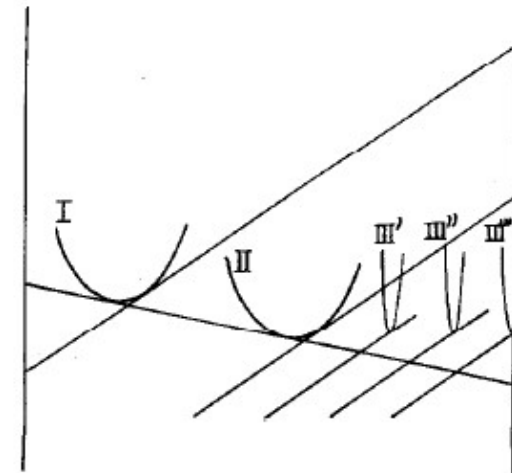


FIGURE 2. Free-energy diagram. The point *o* represents the parent phase. Phase III becomes more favored the more to the right it lies.

Models: Nucleation Rate

ΔG_m : driving force for nucleation

```
Thermo-Calc
Conditions:
T=973.15, W<CR>=0.12, W<C>=1E-2, P=1E5, N=1
DEGREES OF FREEDOM 0

Temperature 973.15 K ( 700.00 C), Pressure 1.000000E+05
Number of moles of components 1.00000E+00, Mass in grams 5.34225E+01
Total Gibbs energy -3.99132E+04, Enthalpy 2.77894E+04, Volume 7.19372E-06

Component      Moles      W-Fraction  Activity   Potential  Ref.stat
C               4.4478E-02 1.0000E-02 1.6563E+00 4.0829E+03 SER
CR             1.2329E-01 1.2000E-01 2.4393E-03 -4.8677E+04 SER
FE             8.3223E-01 8.7000E-01 6.3265E-03 -4.0966E+04 SER

BCC_A2          Status ENTERED      Driving force 0.0000E+00
Moles 1.0000E+00, Mass 5.3422E+01, Volume fraction 1.0000E+00 Mass fractions:
FE 8.70000E-01 CR 1.20000E-01 C 1.00000E-02

CEMENTITE       Status DORMANT      Driving force 1.2737E+00
Moles 0.0000E+00, Mass 0.0000E+00, Volume fraction 0.0000E+00 Mass fractions:
CR 6.38175E-01 FE 2.91769E-01 C 7.00561E-02

M23C6           Status DORMANT      Driving force 1.1359E+00
Moles 0.0000E+00, Mass 0.0000E+00, Volume fraction 0.0000E+00 Mass fractions:
CR 6.03017E-01 FE 3.41486E-01 C 5.54972E-02

M7C3            Status DORMANT      Driving force 1.7049E+00
Moles 0.0000E+00, Mass 0.0000E+00, Volume fraction 0.0000E+00 Mass fractions:
CR 7.62680E-01 FE 1.48159E-01 C 8.91611E-02
POLY_3:
```

Models: Nucleation Rate

Homogeneous nucleation

So far all nucleation theory slides have dealt with homogeneous nucleation of spherical nuclei. Additions to the models must be made in order to take into account:

- Heterogenous nucleation
- Elastic strain energy, resulting in other precipitate shapes

Models: Nucleation Rate

N - Available Nucleation Sites

Homogeneous Nucleation: $N_h = N_A / V_m^\alpha$

Heterogeneous Nucleation - Grain boundaries, edges, corners:

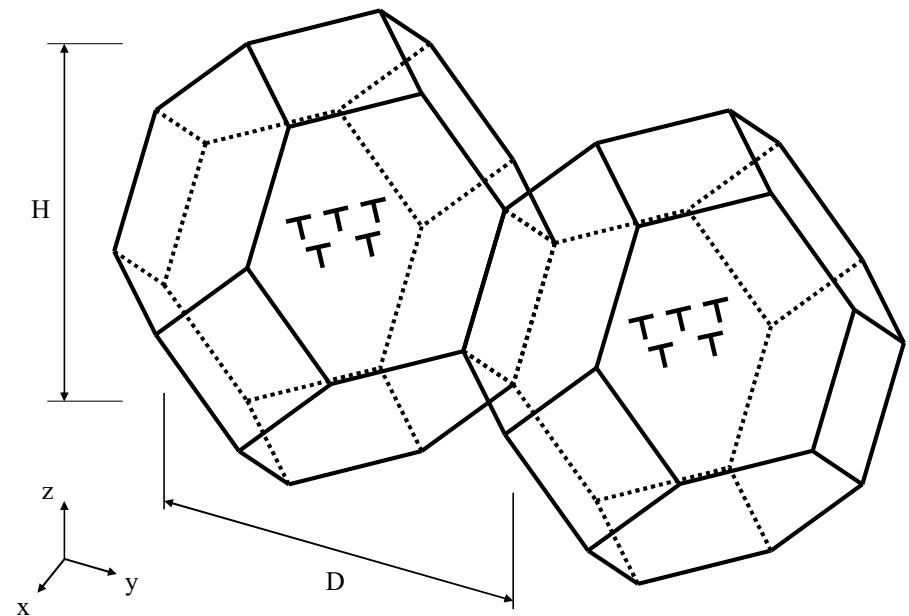
$$\rho_2 = \frac{6\sqrt{1+2A^2} + 1 + 2A}{4A} D^{-1}$$

$$\rho_1 = 2 \frac{\sqrt{2} + 2\sqrt{1+A^2}}{A} D^{-2}$$

$$\rho_0 = \frac{12}{A} D^{-3}$$

$$N_i = \rho_i \left(\frac{N_A}{V_m^\alpha} \right)^{i/3} \quad (i = 2, 1, 0)$$

Aspect Ratio $A=H/D$



Dislocations

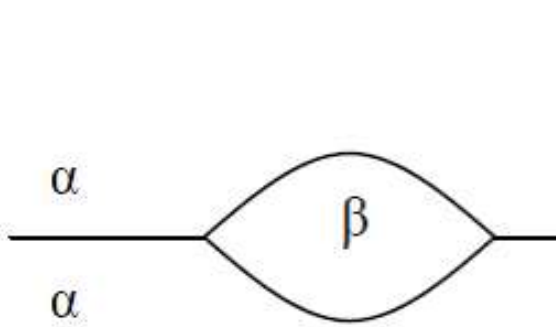
$$N_d = \rho_d \left(\frac{N_A}{V_m^\alpha} \right)^{1/3}$$

Tetrakaidecahedron approximation of grains

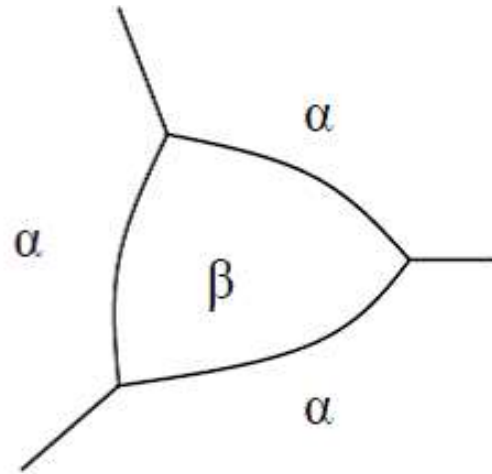
$A=1$, J. Cahn, Acta Metall. 4(1956)449

Models: Heterogenous Nucleation

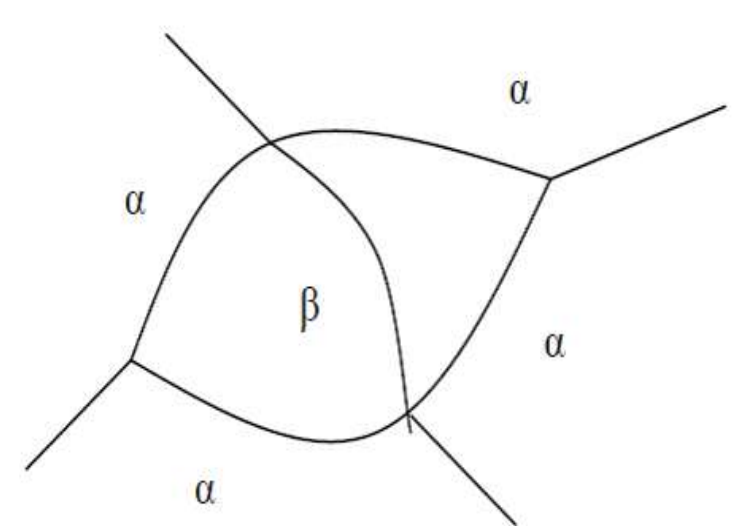
Wetting Angles for Grain Boundary Precipitation



Grain Boundary*
(Two-Grain Junction)



Grain Edge*
(Three-Grain Junction)

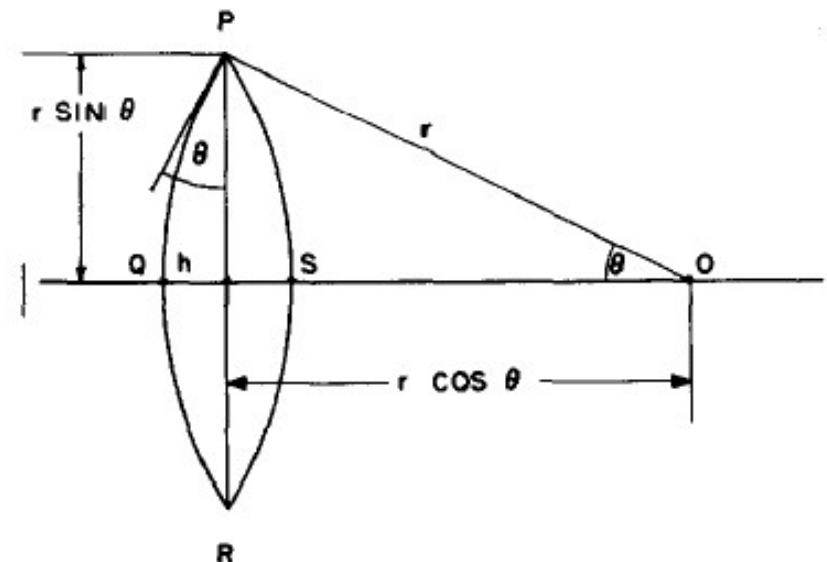


Grain Corner*
(Four-Grain Junction)

* Images taken from L. Zang,
<http://www.eng.utah.edu/~lzang/images/lecture-13.pdf>

Wetting Angle** (Two-Grain Junction)

** Image taken from P. Clemm and J. Fisher, Acta Metallurgica, 3(1)70-73



Models: Heterogenous Nucleation



Shape Factors

Eliminated GB Area	Surface Area of Nuclei	Volume of Nuclei	Wetting Angle
$A_{\alpha\alpha} = ar^2$	$A_{\alpha\beta} = br^2$	$V = cr^3$	$k = \cos \theta = \frac{\sigma_{\alpha\alpha}}{2\sigma_{\alpha\beta}}$

Effects of Wetting Angle

Activation Energy	$W = \frac{4}{27} \frac{\sigma_{\alpha\beta}^3 V_m^2}{(\Delta G_m^{\alpha \rightarrow \beta})^2} \frac{(b - 2ak)^3}{c^2}$
Critical Radius	$r^* = -\frac{2(b - 2ak)\sigma_{\alpha\beta}V_m}{3c\Delta G_m^{\alpha \rightarrow \beta}}$
Zeldovitch Factor	$Z = Z_b \sqrt{\frac{3c}{4\pi}}$
Molecular Attachment Rate	$\beta^* = \frac{br^2 X D}{a^4}$
Nucleation Site Density	$A_{\text{reduction}} = an\bar{r}^2$

The expression of a , b , and c for grain boundary (two-grain junction), grain edge (three-grain junction) and grain corner (four-grain junction) can be found in the paper by P. Clemm and J. Fisher, Acta Metallurgica, 3(1) 70-73.

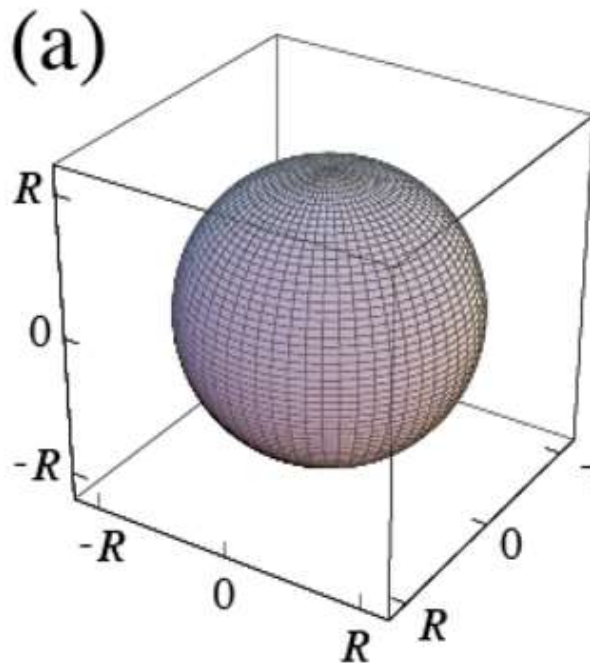
Precipitate Shapes

Elastic strain energy will change the shape of the nucleating particles.

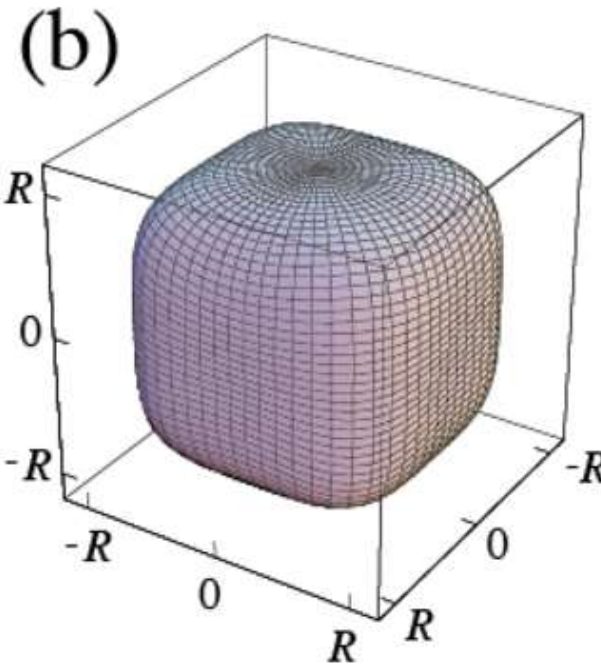
Cuboid (SuperSphere*)

K. Wu, Q. Chen, P. Mason, *J Phase Eq. Diffus.* 39(2018)571-583.

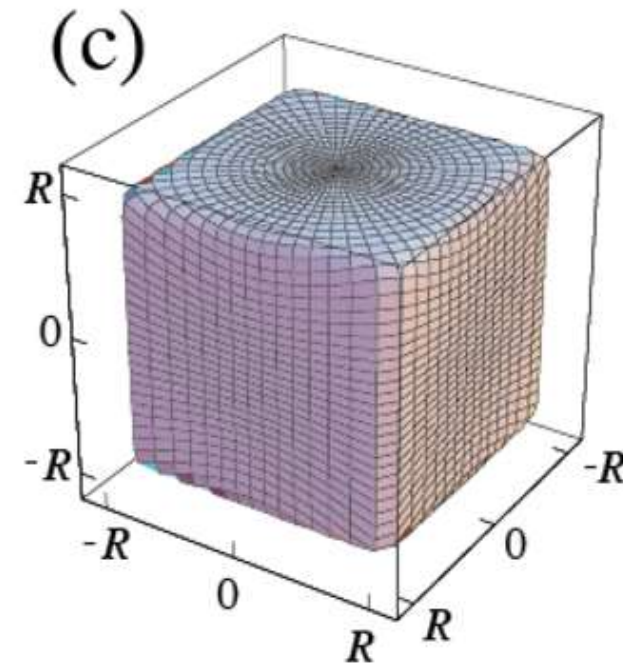
$$\left| \frac{x}{R} \right|^p + \left| \frac{y}{R} \right|^p + \left| \frac{z}{R} \right|^p = 1 \quad (p \geq 2) \quad \eta = 2^{\frac{p-2}{2p}}$$



$$p = 2(\eta = 1)$$



$$p = 4(\eta = 1.19)$$



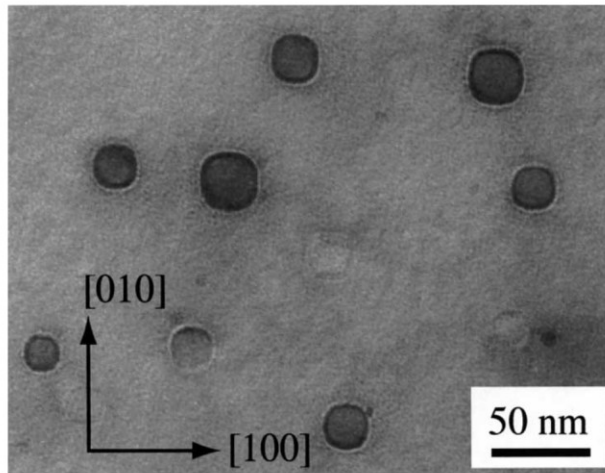
$$p = 20(\eta = 1.37)$$

*Susumu Onaka, *Symmetry* 2012, 4(3), 336-343

Precipitate Shapes

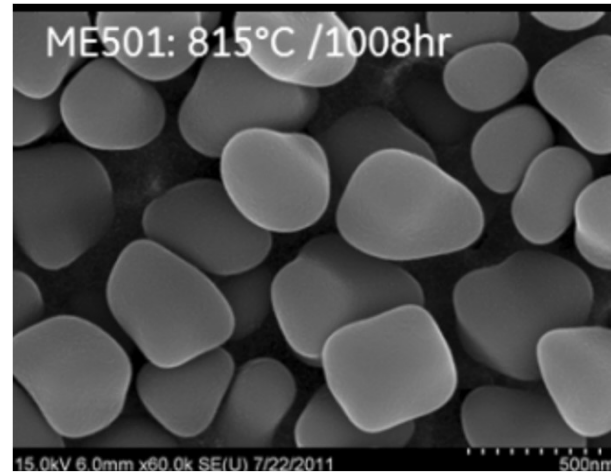
Cuboid (SuperSphere)

CoCr in (Cu)

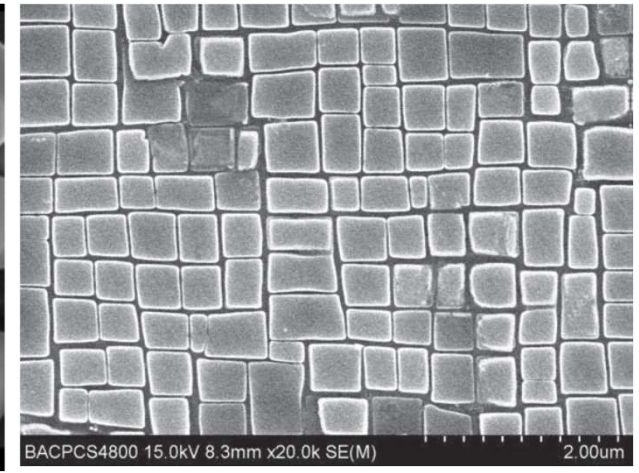


S. Onaka et al., Mater Sci &Engr, A347 (2003) 42 – 49.

γ' Phase in Ni-based Superalloys



A. Powell et al., *Superalloys 2016*, p. 189-196



J.R. Li et al., *Superalloys 2016*, p.57-63

- Alloy chemistry and heat treatment have profound effect on particle morphologies
- Precipitate shape is related to size and atomic misfit
- Precipitate shape is determined automatically by the ratio of interfacial energy/elastic energy

Precipitate Shapes

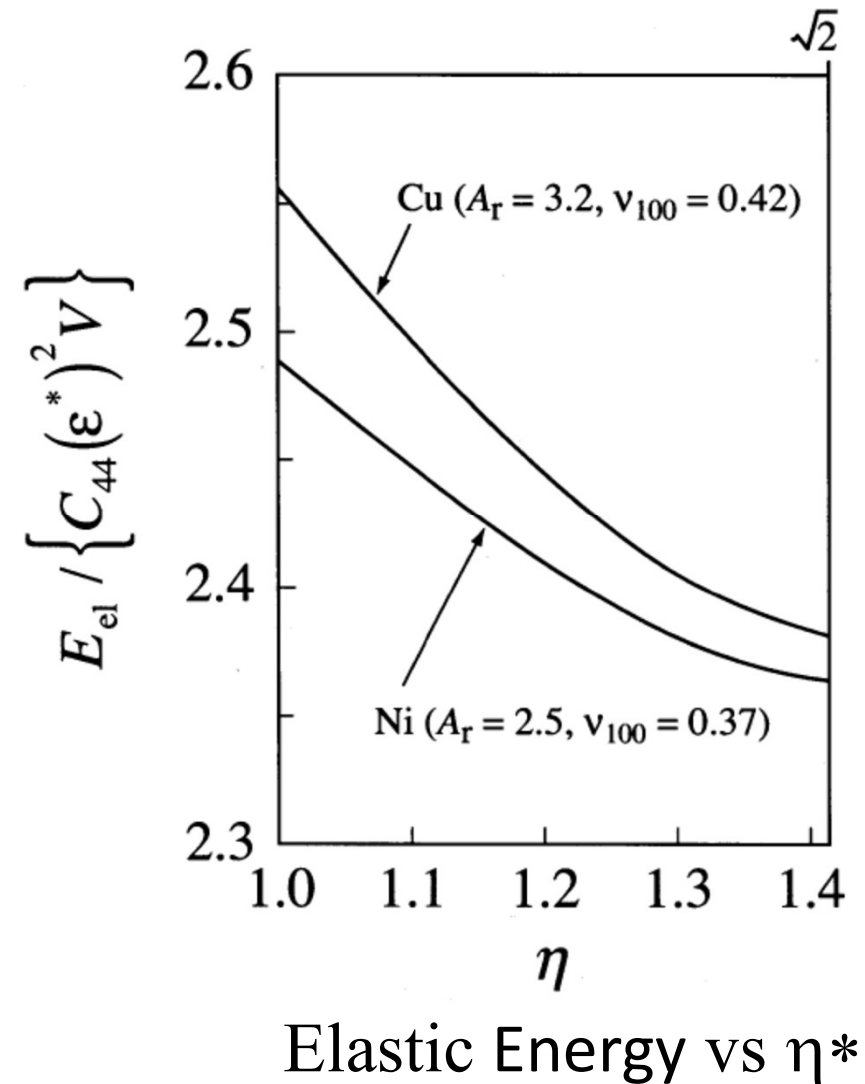
Cuboid (SuperSphere)

➤ Elastic Energy

- Elastically Cubic System
- Strain from Atomic Misfit
- Assumption of Linear Relation up to $\eta=1.35$
- Elastic Energy of Spherical and Cubic Particles from Khachaturyan's Treatment**

➤ Particle Shape

- Determined by Minimization of Combined Interfacial Energy and Elastic Strain Energy



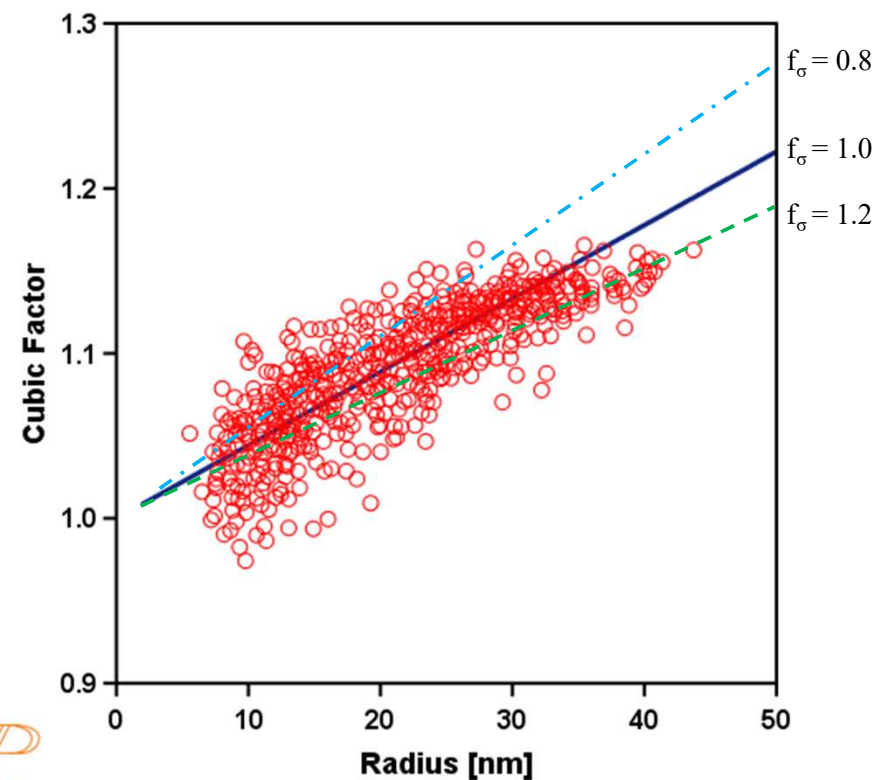
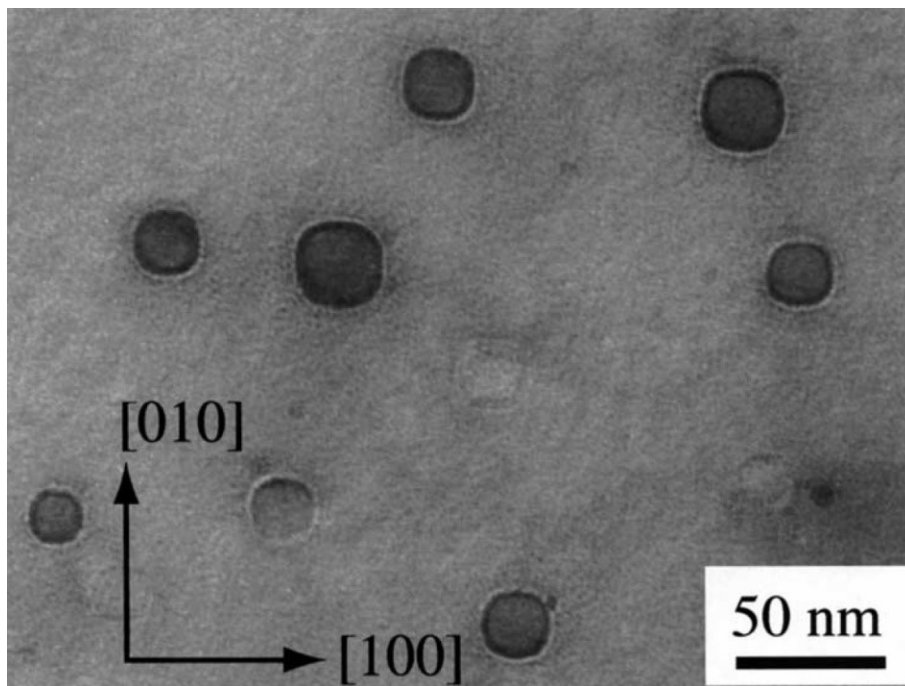
* S. Ontaka et al., *Mater. Sci. Eng.* A347(2003)42

** A.G. Khachaturyan, *Theory of Structural Transformation in Solids*

Calculation – Cu alloys

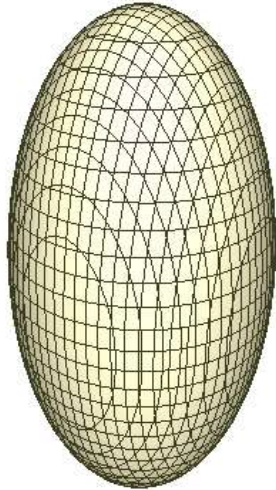
Cu - 1.63wt%Co - 0.41wt%Cr , 973 K

- Databases: TCCU2+MOBCU2
- Cuboid
- Misfit strain from database
- $C_{11}=168.4$, $C_{12}=121.4$, $C_{44}=75.4$ GPa
- Calculated interfacial energy (0.39 J/m²)



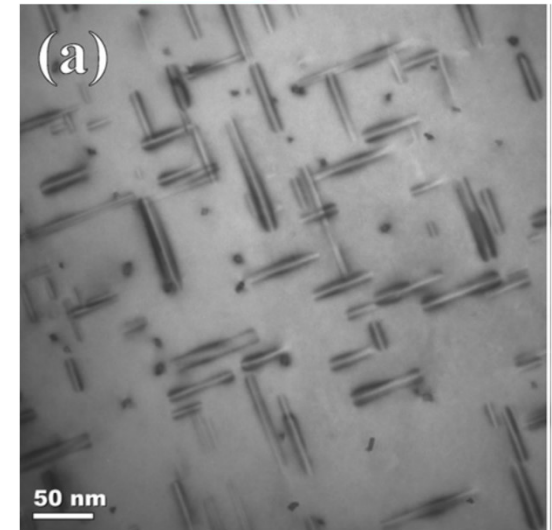
\mathcal{P}

Precipitate Shapes



**Needle
(Prolate Spheroid)**

$$\frac{x_1^2}{r^2} + \frac{x_2^2}{r^2} + \frac{x_3^2}{l^2} \leq 1 \quad l > r$$



β'' phase in Al-Mg-Si Alloy

F.A.Martinsen et al., *Acta Materialia* 60(2012)6091-6101

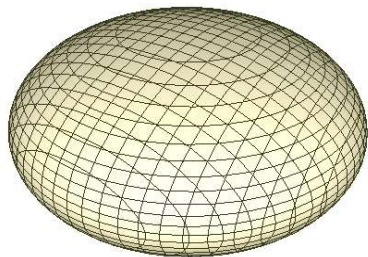
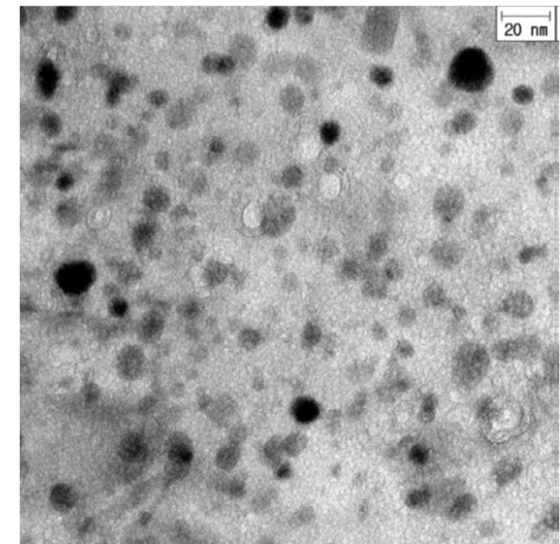


**Plate
(Oblate Spheroid)**

$$\frac{x_1^2}{l^2} + \frac{x_2^2}{l^2} + \frac{x_3^2}{r^2} \leq 1 \quad l > r$$



η' phase in Al-7075 Alloy

M.H.Shaeri et al., *Materials and Design* 57(2014)250-257

- Faster Growth
- Interfacial Energy Anisotropy
- Shape Determined by Ratio of Interfacial Energy/ Elastic Energy

Precipitate Shapes

➤ Interfacial Energy Anisotropy*

$$\frac{\sigma_l}{\sigma_r} = \frac{l}{r} = \alpha$$

➤ Elastic Strain Energy

- Elastically Isotropic or Cubic Systems
- First Approximation: Elastically Homogenous
- Eshelby's Theory**

➤ Particle Shape

- Determined by Minimization of Combined Interfacial Energy and Elastic Energy
- User-Defined, Fixed Value

Needle (Prolate Spheroid)

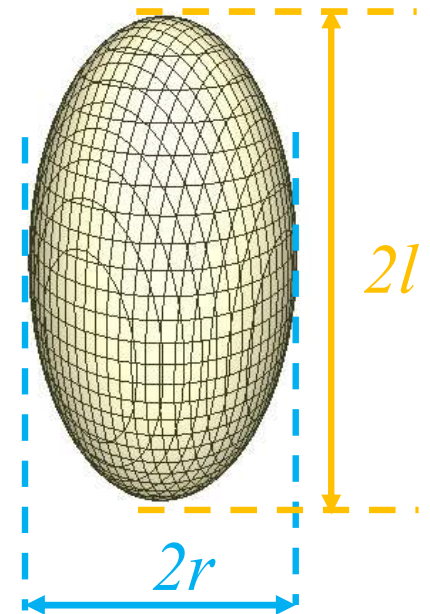
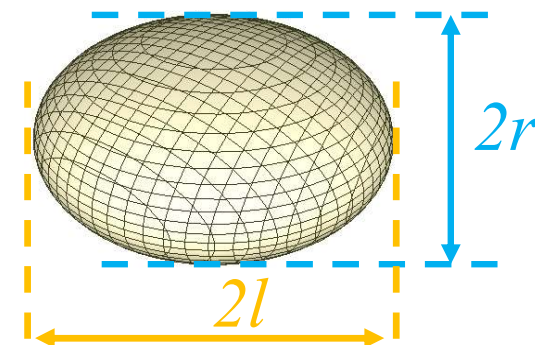


Plate (Oblate Spheroid)



* C.A. Johnson, *Surf. Sci.* 3(1965)429

** J.D. Eshelby, *Pro. Roy. Soc. A*, 241(1957)376

Precipitate Shapes

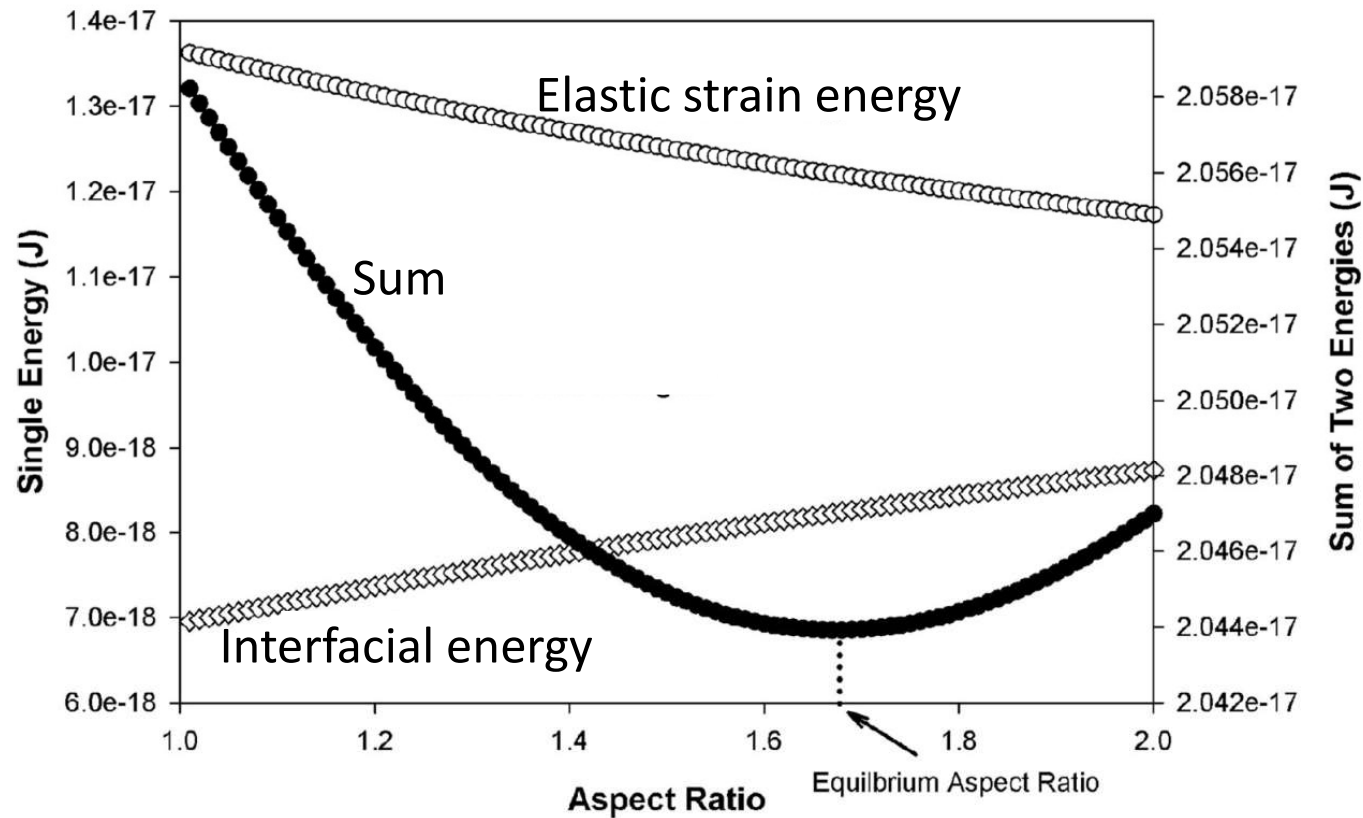


Fig. 1 The calculated elastic strain energy and interfacial energy (with scales displaying on left Y-axis), and the sum of the two energies (with scale displaying on right Y-axis) as function of aspect

ratio for a Cu_4Ti particle. The volume of the particle is equal to a sphere with radius of 4 nm. The minimum of the summed energy determines the equilibrium aspect ratio

Examples

Cu-Ti

TC-PRISMA Examples

Example, Cu-Ti Alloy:

Precipitation of Cu_4Ti from FCC (Kampmann et al 1987)

Precipitation Kinetics in Metastable Solid Solutions – Theoretical Considerations and Application to Cu-Ti Alloys

R. Kampmann, H. Eckerlebe, and R. Wagner

GKSS-Forschungszentrum, Institut für Physik
D-2054 Geesthacht, FR Germany

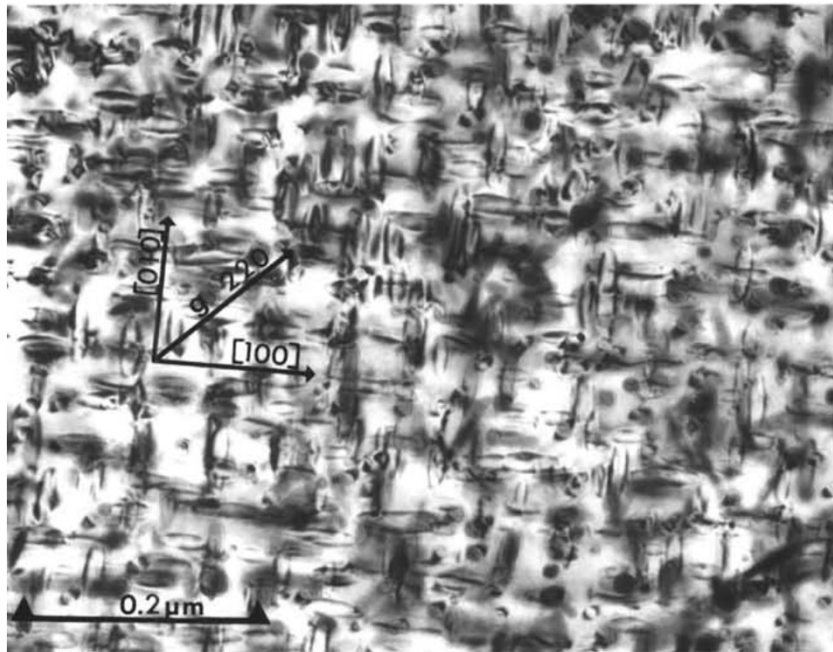
ABSTRACT

Cu-2.9 at.% Ti single crystals were homogenized at various temperatures ($780^\circ\text{C} \leq T_H \leq 960^\circ\text{C}$) and quenched. Subsequent isothermal aging at 350°C led to phase separation, the kinetics of which have been followed by employing small-angle neutron scattering (SANS). According to complementary transmission electron and analytical field ion microscopy studies, the resulting transformation products of this first order phase transition are stoichiometrically ordered ellipsoidal Cu_4Ti particles, the aspect ratio of which changes with aging time (t) as revealed by two-dimensional SANS-detection. In the early stages of phase separation, the decomposition kinetics are strongly influenced by the quenching rate via quenched-in excess vacancies. During aging the structure factor $S(\kappa, t)$ develops a maximum, the height (S_m) of which increases and the position (κ_m) of which decreases with t . Neither $S_m(t)$ nor $\kappa_m(t)$ follow a power law as predicted by several recent theories on spinodal decomposition. On the other hand, the time evolution of the mean Ti-rich cluster size (\bar{R}), their number density (N_v), and the supersaturation (Δc) as inferred from the SANS-data and the diffuse Laue-scattering, are well predicted by a precipitation model which describes nucleation, growth and coarsening as competing processes.

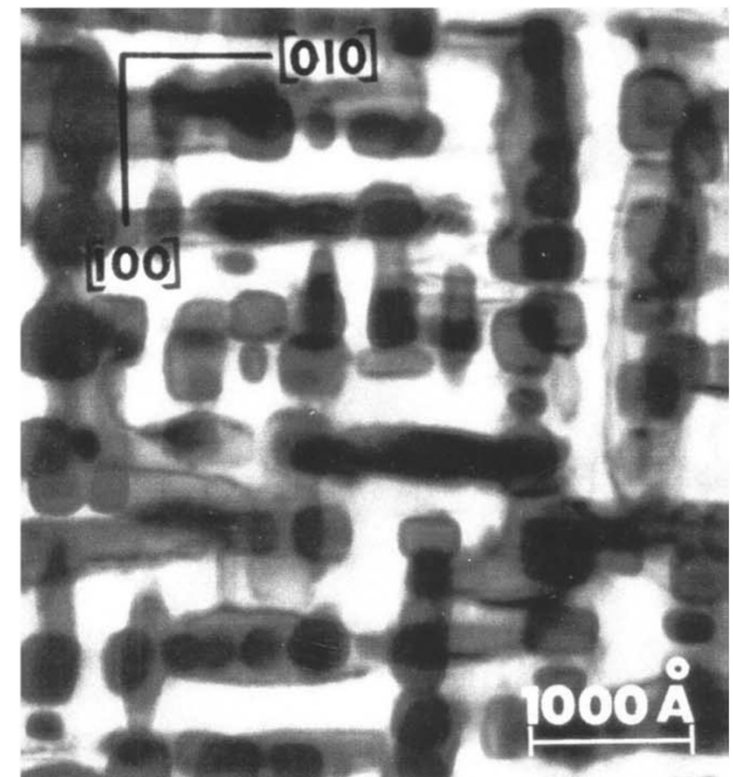
TC-PRISMA Examples

Example, Cu-Ti Alloy:

Precipitation of Cu_4Ti
from FCC



Cu-1wt.%Ti, 500°C, 100min



Cu-4wt.%Ti, 500°C, 2000min

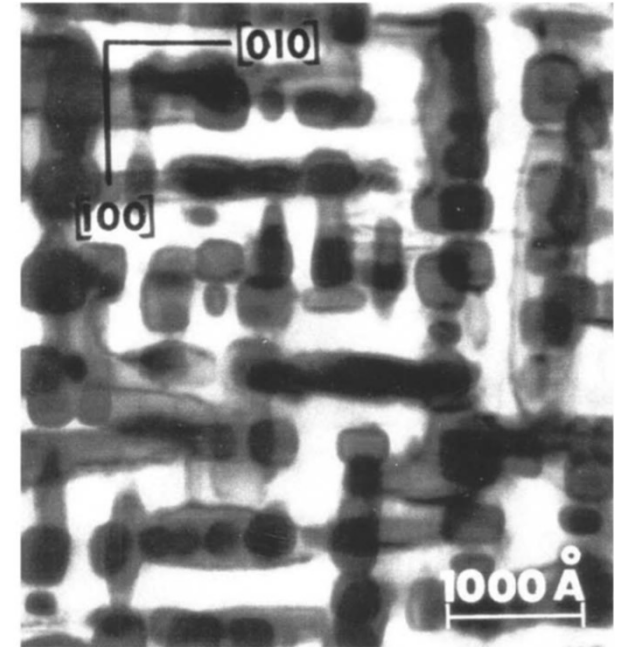
Examples: Cu-Ti Alloy

Precipitation of Cu_4Ti from FCC

- Needle shape
- Tetragonal body-center D1a
- Coherent with matrix with a tetragonal misfit*

$$\epsilon_{11} = \epsilon_{22} = 0.022 \quad [100]_{\text{FCC}}, [010]_{\text{FCC}}$$

$$\epsilon_{33} = 0.003 \quad [001]_{\text{FCC}}$$



Cu_4Ti precipitates in a Cu-Ti Alloy

Image taken from W.A.Soffa and D.E. Laughlin, *Prog. Mater. Sci.* 49(2004)347

* C. Borchers, *Phil. Mag.*, 79(1999)537

Example Cu-Ti Alloy

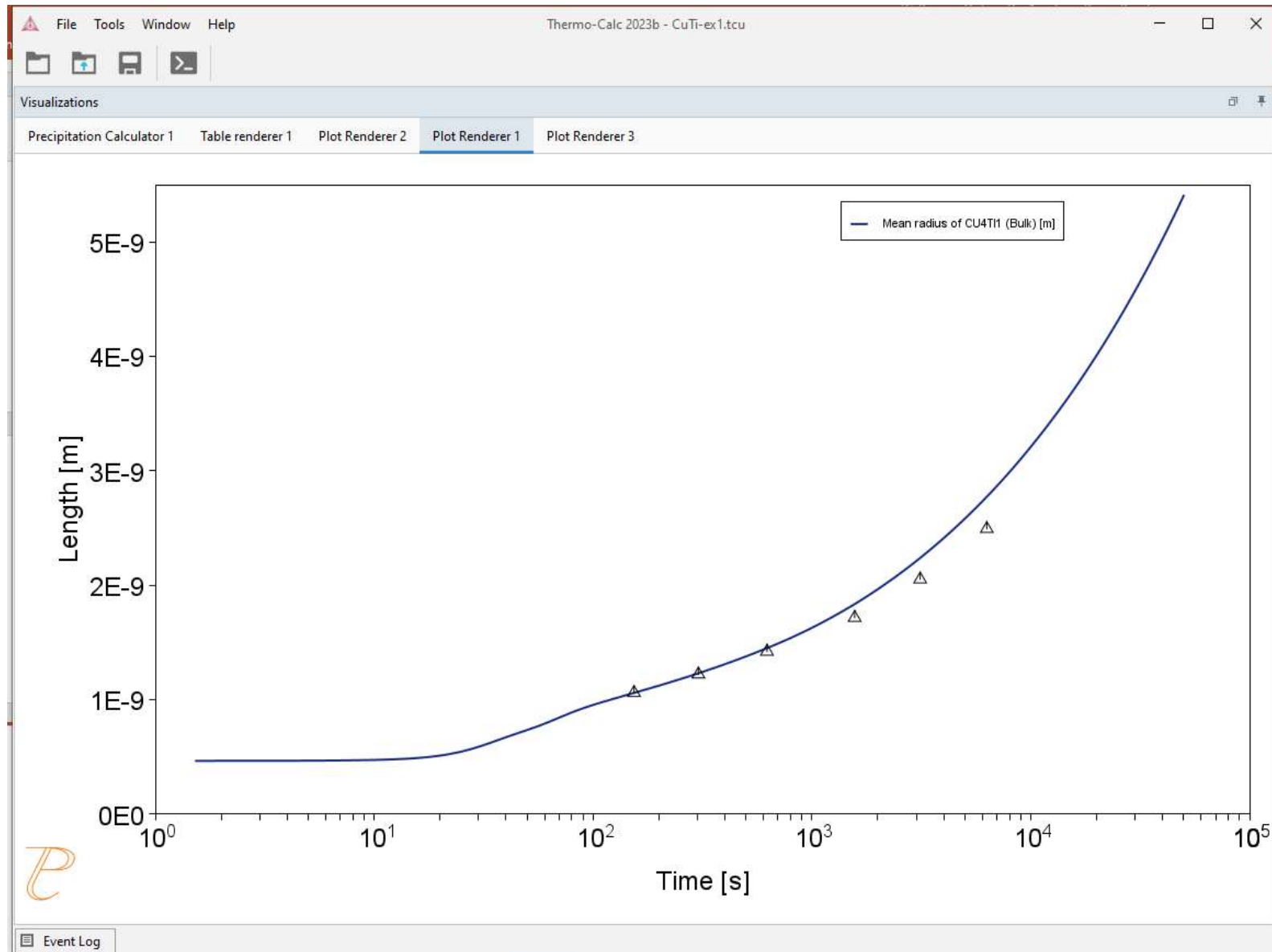
Precipitation of Cu_4Ti from FCC (Cu) (Kampmann et al 1987) . They estimated $D = 2.5 \cdot 10^{-19} \text{ m}^2/\text{s}$ after solution treatment and quenching. Compare with our calculated D value.

Composition	Cu - 1.9 Ti (at. %)
Temperature	350 °C
Simulation time	1E4 s
Nucleation Site Type	Bulk
Interfacial Energy	0.067 J/m ²
Mobility Adjustment	100
Molar volume of Phases	Database values

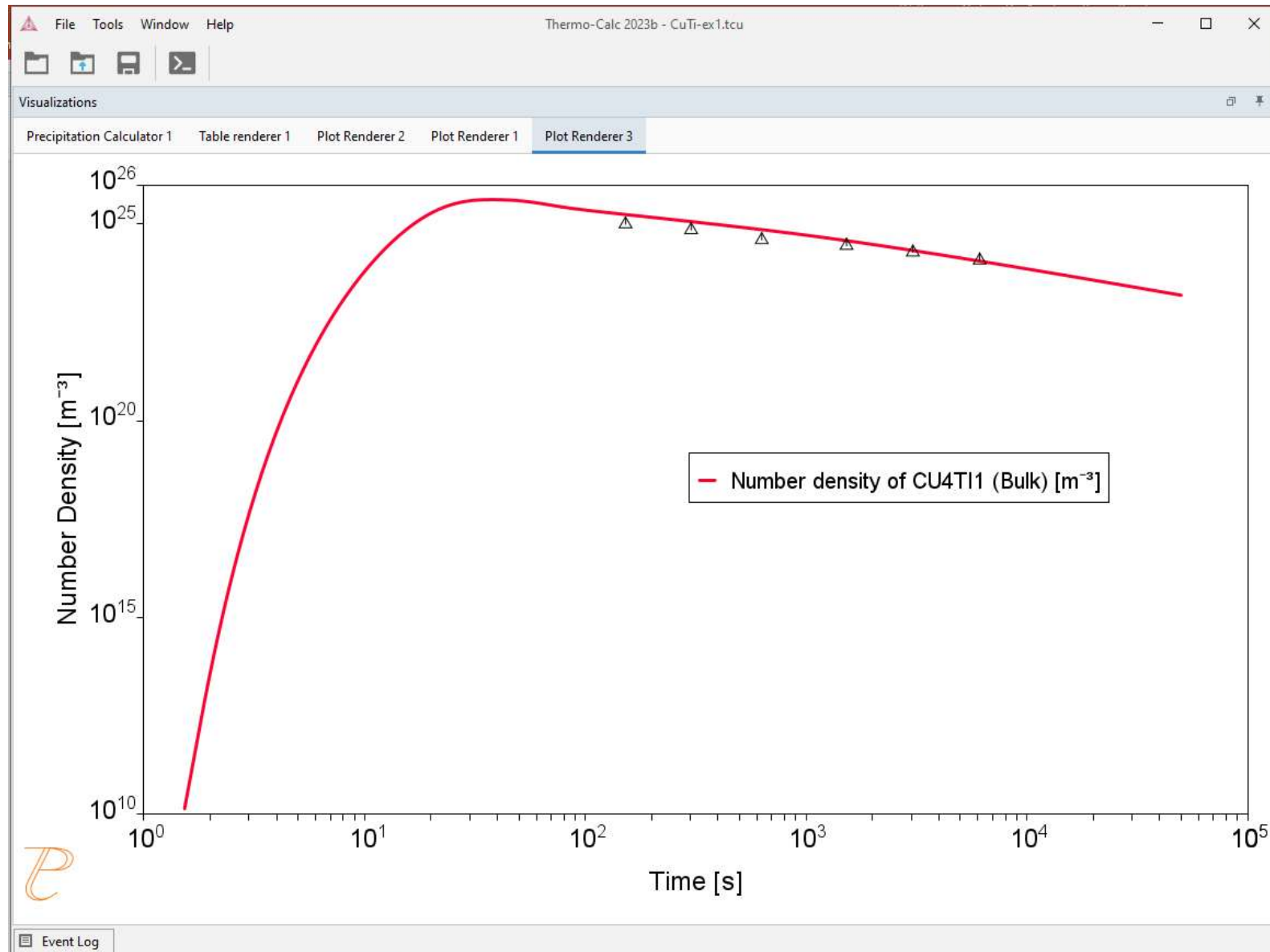
Cu-Ti Example 1

System	
Database package	TCCU6 + MOBCU5
Elements	Cu, Ti
Matrix phase	FCC_A1
Precipitate phase	Cu ₄ Ti
Conditions	
Composition	Cu - 1.9 Ti (at. %)
Temperature	350 °C
Simulation time	5E4 s
Nucleation properties	Nucleation Site Type: Bulk
Data Parameters	
Interfacial Energy	Bulk: 0.067 J/m ²
Molar Volume (Matrix):	FCC: Database
Molar Volume (Precipitate):	Cu ₄ Ti: Database
Mobility Adjustment Factor	100

Cu-Ti Example 1



Cu-Ti Example 1



Cu-Ti Example 2 – needle shape

System	
Database package	TCCU6 + MOBCU5
Elements	Cu, Ti
Matrix phase	FCC_A1
Precipitate phase	Cu ₄ Ti
Conditions	
Composition	Cu - 1.9 Ti (at. %)
Temperature	350 °C
Simulation time	1E5 s
Nucleation properties	Nucleation Site Type: Bulk
Data Parameters	
Interfacial Energy	0.067 J/m ²
Molar Volume (Matrix):	Database
Molar Volume (Precipitate):	Database
Mobility Enhancement Factor	100

Cu-Ti Example 2 – needle shape

Precipitation of Cu_4Ti from FCC

- Cu-1.9at.% Ti
- Databases:
TCCU6+MOBCU5 (or demo-DB)
- User-input misfit strain

ϵ_{11}	ϵ_{22}	ϵ_{33}
0.022	0.022	0.003

* C. Borchers, *Phil. Mag.*, 79(1999)537

C_{11}	C_{12}	C_{44}
168.4 GPa	121.4 GPa	75.4 GPa

* J.K. Lee et al., *Metall. Trans. A*, 8(1977)963

- Default values for other parameters

Cu-Ti Example 2 – needle shape

Visualizations



Plot Renderer 2

Plot Renderer 1

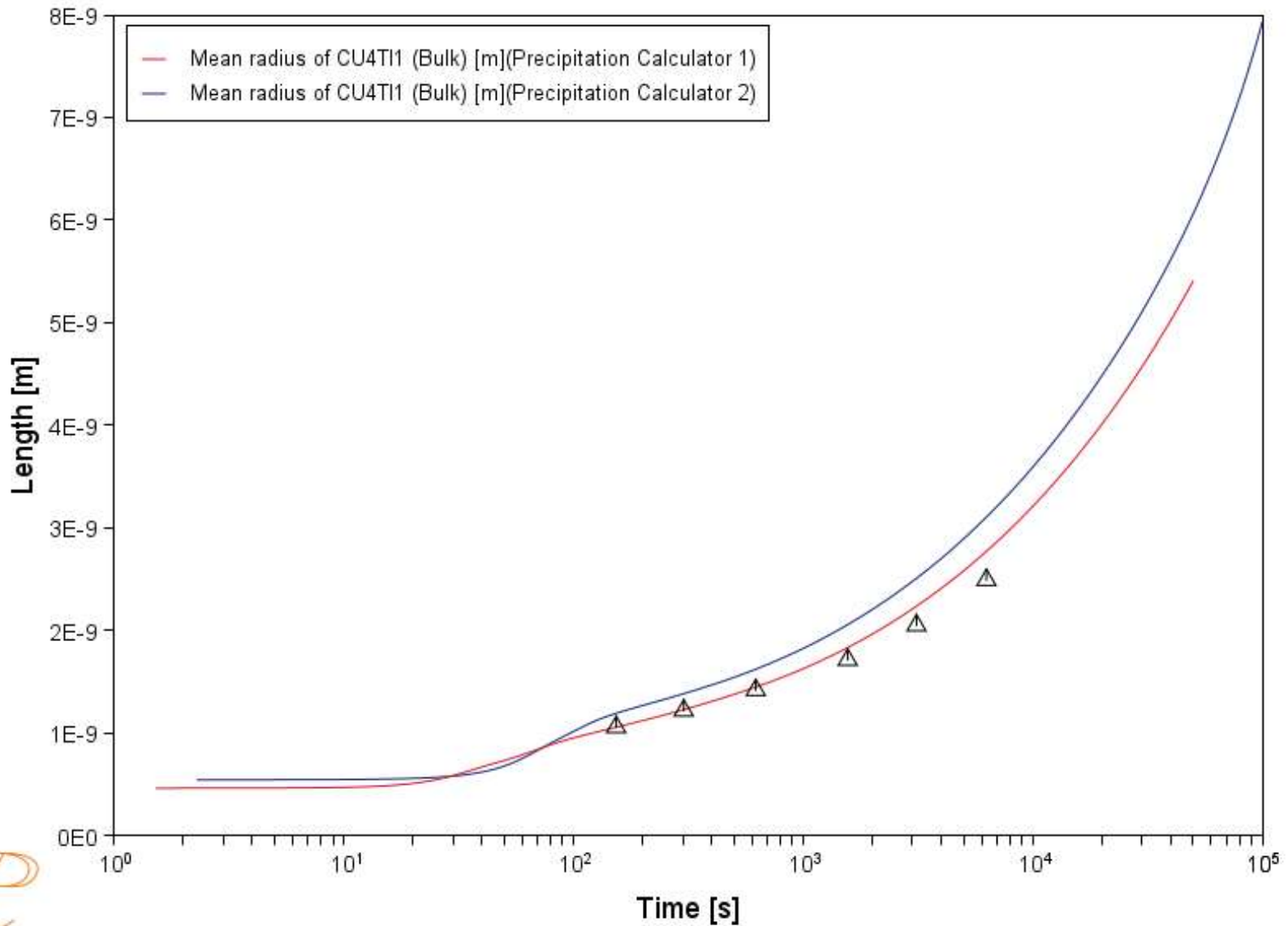
Plot Renderer 3

Plot Renderer 4

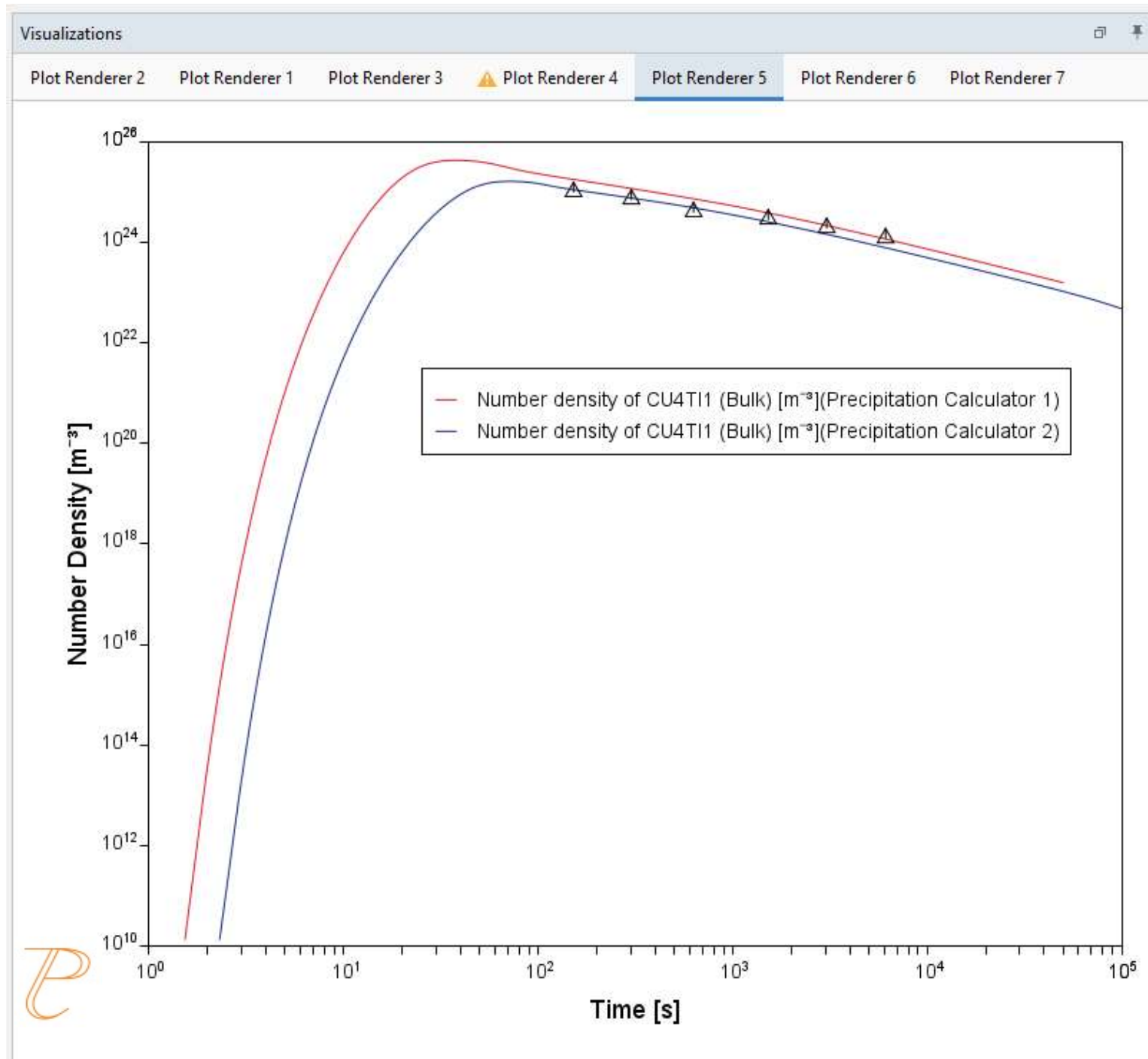
Plot Renderer 5

Plot Renderer 6

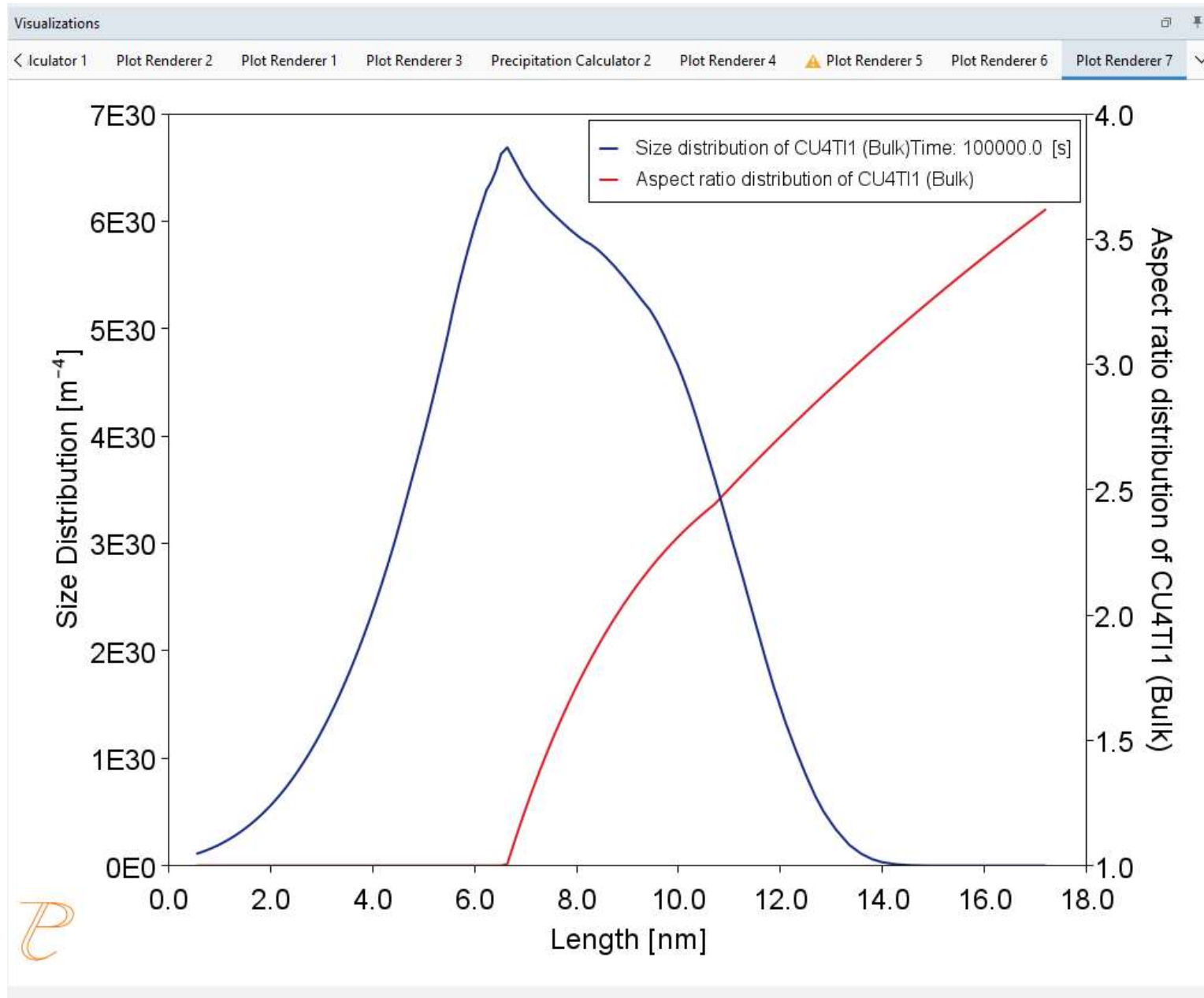
Plot Renderer 7



Cu-Ti Example 2 – needle shape



Cu-Ti Example 2 – needle shape



Cu-Ti Example 3 – TTP diagram

System	
Database package	CUDEMO + MUCUDEMO
Elements	Cu, Ti
Matrix phase	FCC_A1
Precipitate phase	CU4TI1
Conditions – TTT diagram	- Phase fraction = 0.001
Composition	Cu - 1.9 Ti (at. %)
Temperature	200 °C - 570 °C, $\Delta=10$ °C
Max annealing time	1E7 s
Nucleation properties	Nucleation Site Type: Bulk
Data Parameters	
Interfacial Energy	0.067
Molar Volume (Matrix):	Database
Molar Volume (Precipitate):	Database
Mobility Enhancement Factor	100

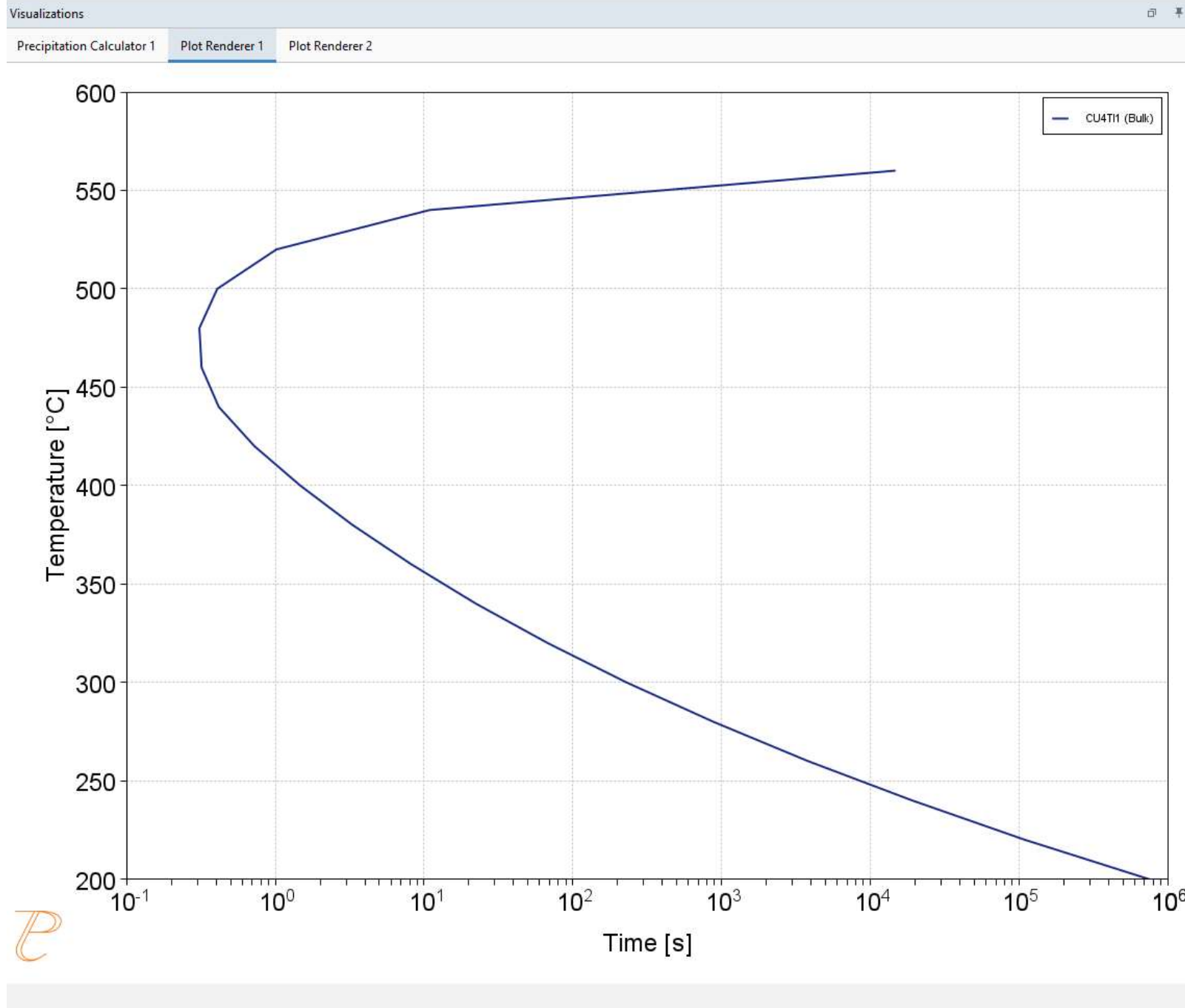
Set Options:

Number of grid points: 15

Maximum number of grid points: 20

Minimum number of grid points: 10

Cu-Ti Example 3 – TTP diagram



Q & A